



ANNUAL RESEARCH REPORT

2022

for projects conducted in 2021

Gary S. Was, Director
George Jiao, Manager and Accelerator Scientist
Fabian Naab, Senior Accelerator Scientist
Prashanta Niraula, Accelerator Scientist
Robert Hensley, Electronic Systems Engineer

2600 Draper Road
Department of Nuclear Engineering and Radiological Sciences
University of Michigan
Ann Arbor, Michigan 48109-2145
mibl.engin.umich.edu

Telephone: (734) 936-0131

Fax: (734) 764-8060

The Annual Research Report

This report summarizes the principal research activities in the Michigan Ion Beam Laboratory during the past calendar year. One hundred and fourteen researchers conducted 42 projects at MIBL that accounted for 182 irradiations and 5,481 hours of instrument time. The programs included participation from researchers at the University, other universities across the United States, corporate research laboratories, private companies, government laboratories, and various international organizations. These projects also included 8 projects funded through the Nuclear Science User Facility program. The extent of participation of the laboratory in these programs ranged from routine surface analysis to triple beam irradiations. Experiments included Rutherford backscattering spectrometry, elastic recoil spectroscopy, nuclear reaction analysis, direct ion implantation, ion beam mixing, ion beam assisted deposition, and radiation damage by proton irradiation and self-ion irradiation, dual ion irradiation and triple beam irradiation, irradiation accelerated corrosion, and irradiation creep. The following pages contain a synopsis of the research conducted in the Michigan Ion Beam Laboratory during the 2021 calendar year.

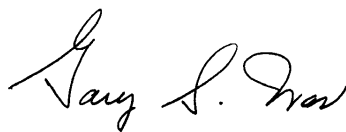
About the Laboratory

The Michigan Ion Beam Laboratory for Surface Modification and Analysis was completed in October of 1986. The laboratory was established for the purpose of advancing our understanding of ion-solid interactions by providing up-to-date equipment with unique and extensive facilities to support research at the cutting edge of science. Researchers from the University of Michigan as well as industry and other universities are encouraged to participate in this effort.

The lab houses a 3 MV Pelletron accelerator, a 1.7 MV tandem ion accelerator, and a 400 kV single ended ion accelerator that are configured to provide for a range of ion irradiation and ion beam analysis capabilities utilizing 9 beamlines, 5 target chambers and a transmission electron microscope coupled to two beamlines to provide dual beam irradiation in-situ in the TEM. The control of the parameters and the operation of these systems are mostly done by computer and are interconnected through a local area network, allowing for complete control of irradiations from the control room as well as off-site monitoring and control.

In 2010, MIBL became a Partner Facility of the National Scientific User Facility (NSUF), based at Idaho National Laboratory, providing additional opportunities for researchers across the US to access the capabilities of the laboratory. In 2016, MIBL was recognized as the top ion beam laboratory in the U.S. by the Nuclear Science User Facilities program.

Respectfully submitted,

A handwritten signature in black ink, appearing to read "Gary S. Was". The signature is fluid and cursive, with the first name "Gary" being more prominent.

Gary S. Was, Director

RESEARCH PROJECTS

Nuclear Science User Facility (NSUF) Projects

THE ROLE OF PRECIPITATE COHERENCY ON HELIUM TRAPPING IN ADDITIVELY MANUFACTURED ALLOY 718

S. Taller¹, T. Lach², K. Sun³

¹Nuclear Energy and Fuel Cycle Division, Oak Ridge National Laboratory

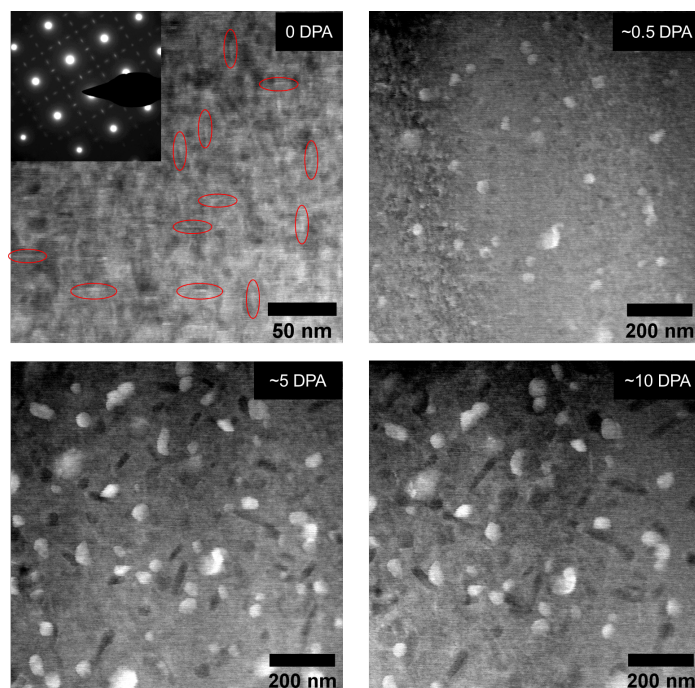
²Materials Science and Technology Division, Oak Ridge National Laboratory

³Department of Materials Science and Engineering, University of Michigan

Ni-based superalloys are a candidate alloy class for advanced reactor applications because of their intrinsic resistance to creep, adequate corrosion resistance and the ability to tailor the microstructure for high strength possibly through additive manufacturing. These high strength Ni-based alloys gain their strength mostly through secondary precipitating phases in the lattice, such as the intermetallic phases δ , γ' or γ'' . The absorption of transmutation-produced helium at grain boundaries at high temperature becomes a key factor in the propagation of cracks, possibly leading to subcritical crack growth. The precipitate-lattice interfaces can act as benign locations in the microstructure to trap helium – possibly controlled by the degree of coherency – reducing the detrimental accumulation of helium and formation of cavities at boundaries.

Two heats of Ni-superalloy Inconel 718 with large pre-existing precipitate densities with varying coherency were evaluated using the in-situ dual ion irradiation capability within the 300 kV FEI Tecnai transmission electron microscope at the Michigan Ion Beam Laboratory. Irradiations were conducted up to 10 dpa at $0.6\text{--}1.1 \times 10^{-3}$ dpa/s using 1.17 MeV Kr ions with ~ 400 appm He/dpa co-injected from 23 keV He ions at temperatures from 500-700°C. High angle annular dark field (HAADF) images were continuously collected during each irradiation to capture the time-dependent evolution of the microstructure. Dissolution of pre-existing γ'' precipitates occurred early (<1 dpa) for all conditions. At 500 °C, small cavities nucleated by 1 dpa, and a phase with similar contrast to γ'' emerged at about 5 dpa. At 600 °C and 700 °C, both cavity nucleation and precipitate dissolution and reemergence were accelerated. Further analysis will be conducted to identify the emerged phase or phases and quantify the irradiated microstructure.

This work was supported by the U.S. Department of Energy, Office of Nuclear Energy under DOE Idaho Operations Office Contract DE-AC07-051D14517 as part of a Nuclear Science User Facilities experiment.



STEM HAADF images of the microstructure from dual ion irradiation of one heat of additively manufactured Inconel 718 with 1.17 MeV Kr and 23 keV He ions at 600°C. The bright features are Nb-rich precipitates and cavities can be observed as dark features. At 0 dpa, the γ'' precipitates (highlighted with red ovals) form a superlattice and dissolved early. Features believed to be cavities nucleated by 0.5 dpa and elongated along preferred planes with continuing irradiation up to 10 dpa.

SCC IN Fe-BASED WELDMENTS FOR LWR SUSTAINABILITY

B.J. Heuser,¹ X. Bai,² B. Spencer,³ and G.S. Was⁴

¹ Department of Nuclear, Plasma, and Radiological Engineering, University of Illinois

² Department of Materials Science and Engineering, Virginia Tech

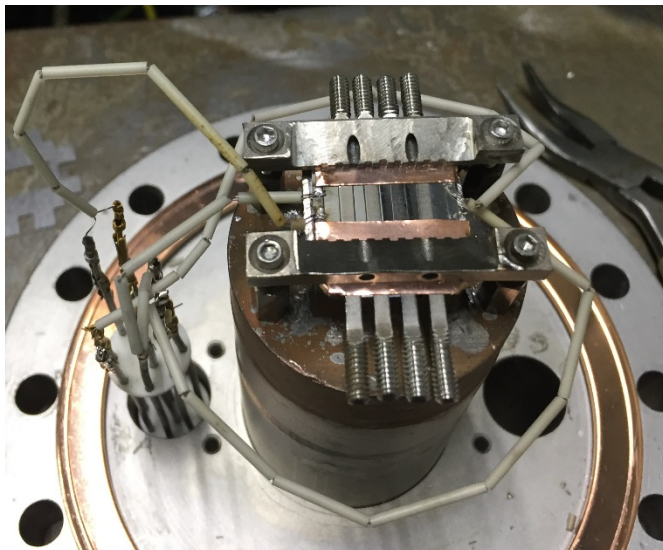
³ Fuels Modeling & Simulation, Idaho National Laboratory

⁴ Department of Nuclear Engineering & Radiological Sciences, University of Michigan

The objective of this project is to provide experimental data on the performance of Alloy 308/309 weldments during exposure to environmental factors typical of normal LWR operation in support of the LWRS Program. In particular, the work scope is designed to determine inter-granular stress corrosion cracking (IGSCC) susceptibility with respect to radiation damage and LWR primary coolant chemistry. The goal is to correlate crack initiation and IGSCC to 1) grain boundary orientation, 2) local grain boundary chemistry and oxidation, 3) and localized deformation, and 4) dpa displacement cascade damage. The experimental protocols are designed to separate the effect of irradiation and associated radiation damage from environmental factors such as LWR water chemistry and applied load and to determine the synergistic effect of irradiation, water chemistry, and tensile stress. In addition, modeling activities are proposed that capture salient features of the materials response of these alloys to LWR environments. The combined experimental and computational methodology is anticipated to improve the predictive capability of Grizzly using a novel extended finite element method (XFEM). The proposed project will be supportive to the LWRS Program in two ways. First, it will expand the knowledge base to include the behavior of weldments found in LWRs. Second, it will serve as input into a modeling component to this project, which in turn will lead to enhanced predictive capability of Grizzly.

We have performed extensive SSR immersion testing of an EPRI SA508-304L weldment under BWR-NWC conditions using the UIUC recirculating loop autoclave. In addition, the four sets of proton irradiation experiments were performed at the MIBL between October 2018 and July 2021. The figure below shows four tensile specimens and six TEM specimens mounted prior to the irradiation experiment. These specimens were successfully irradiated at 360 °C to approximately 5 dpa (quick K-P model calculation via TRIM at 60% of the Bragg peak).

This work was supported by the U.S. Department of Energy, Nuclear Energy University Programs under contract DE-NE0008699.



Mounted tensile and TEM specimens prior to proton irradiation at 360°C.

IN-SITU AND EX-SITU INVESTIGATIONS OF IRRADIATION DAMAGE IN NANOSTRUCTURED ODS HIGH-ENTROPY ALLOYS

X. Zhang¹, F. Wang¹, B. Cui¹, Z. Jiao², K. Sun², O. Toader², G.S. Was²

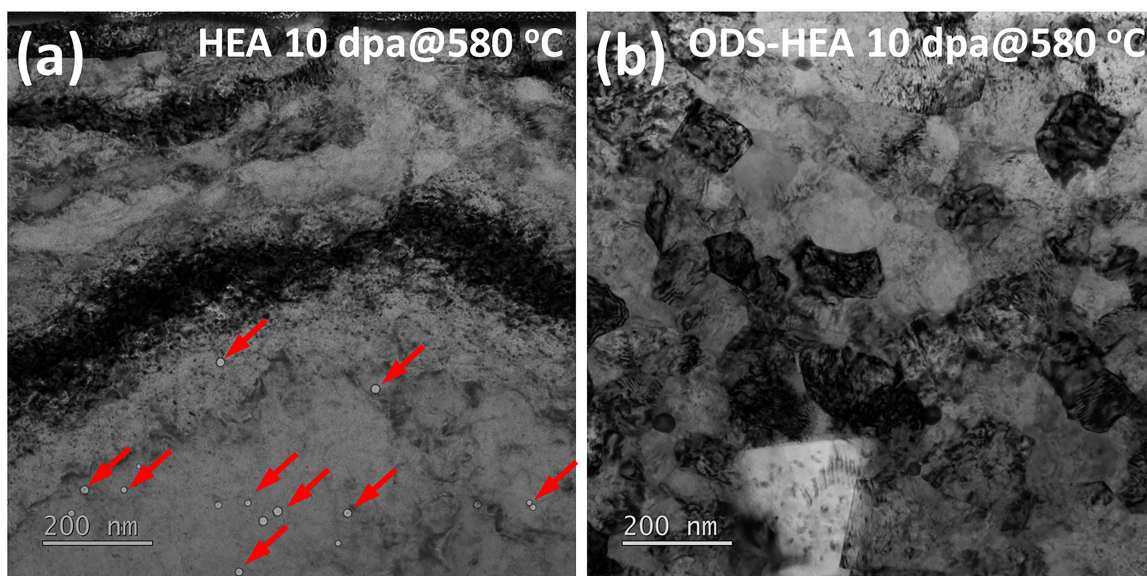
¹Department of Mechanical and Materials Engineering, University of Nebraska-Lincoln

²Department of Nuclear Engineering and Radiological Sciences, University of Michigan

The objective of this RTE project is to use the *in situ* and *ex situ* dual ion irradiation experiments to investigate the irradiation damage in nanostructured oxide-dispersion-strengthened (ODS) high-entropy alloys (HEAs) at elevated temperatures. The homogenous dispersion of nanometer-size oxide particles in the HEA matrix may retard the dislocation and reduce grain coarsening, thus increasing the high-temperature strength and creep resistance of HEAs. This RTE project has used dual ion irradiation and electron microscopy characterizations to examine the fundamental irradiation damage mechanisms, and thus evaluate ODS-HEAs as the potential structural materials for fast reactors.

NiCoCrMnFe HEA (named as HEA) and ODS NiCoCrMnFe HEA (named as ODS-HEA) samples were fabricated by spark plasma sintering (SPS). The samples for *in situ* transmission electron microscopy (TEM) dual irradiation experiments were extracted using the focused ion beam (FIB) method and then transferred to nano chips. The samples for *ex situ* irradiation experiments were machined to the dimensions of 10×15×2 mm. The irradiation conditions were: 5 MeV Fe ion irradiation to 0, 1 and 10 dpa; 25, 400, and 580 °C; and 20 ppm helium per dpa. TEM analysis was also conducted in the *ex situ* irradiated samples, which were extracted from the 600 to 1000 nm depth from the surface by FIB. TEM characterizations (figure) show that voids (with an average diameter of 11 nm) were formed in HEA with damage level of 10 dpa and 20 ppm He at 580 °C, while no voids were observed in ODS-HEA, suggesting a significant improvement of void swelling resistance. More details will be available in the future journal article.

This work was supported by the U.S. Department of Energy, Office of Nuclear Energy under DOE Idaho Operations Office Contract DE-AC07-051D14517 as part of a Nuclear Science User Facilities experiment, and the Nuclear Regulatory Commission Faculty Development Grant (No. 31310018M0045)



Comparison of microstructures of (a) HEA and (b) ODS-HEA with damage level of 10 dpa and 20 ppm He at 580 °C. Voids are indicated by arrows.

COMPOSITIONALLY GRADED SPECIMEN MADE BY LASER ADDITIVE MANUFACTURING AS AN HIGH-THROUGHPUT METHOD FOR NUCLEAR ALLOY DISCOVERY

X. Lou¹, J. Yang¹, L. Hawkins², L. He², M. Song³, Y. Zhang⁴, D. Schwen³

¹Department of Mechanical Engineering, Auburn University

²Idaho National Laboratory

³Department of Nuclear Engineering and Radiological Sciences, University of Michigan

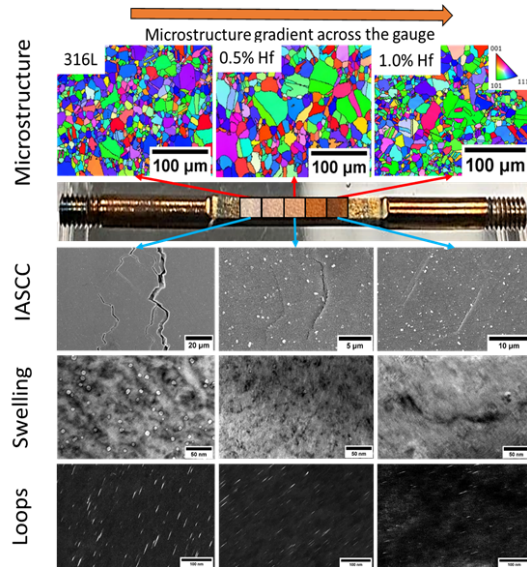
⁴Engineering Physics Department, University of Wisconsin

This study demonstrates the feasibility of using compositionally gradient specimens, fabricated by laser additive manufacturing (AM) and post-AM thermo-mechanical treatment, to accelerate alloy synthesis, radiation experiment, and the assessment of irradiation properties in light water reactor environments. The effects of minor transition metal element doping in austenitic 316L stainless steel (SS) was selected as the topic of interest. By comparing to the data in literature, we confirmed that the compositionally graded specimen produces the same trend of void swelling, dislocation loops, radiation-induced segregation (RIS), radiation hardening, and irradiation-assisted stress corrosion cracking (IASCC) susceptibility as the wrought specimen produced by cast/forging process.

Optomec LENS 500 DED AM system was used to fabricate compositionally graded specimens with Hf, Ta, Y, Ti, Zr gradient, and their combination. To simulate the wrought grain structure, post-AM thermo-mechanical treatment was necessary to transform the as-built AM structure into the recrystallized equiaxed grains. Recrystallization was achieved by cold rolling and solution annealing. Both tensile and TEM samples were machine-finished. Before radiation, the irradiated face of the samples was first ground down to 800 grits by SiC papers, and then electropolished in the methanol solution with 10 vol% perchloric acid at 40 V under -30°C for 30 s. The radiation was conducted using a 3 MV National Electronics Corporation Pelletron accelerator in the Michigan Ion Beam Laboratory (MIBL) at the University of Michigan. The samples were irradiated using 2 MeV protons under 360°C . A damage level of 2.5 dpa (Kinchin-Pease calculation) at $\sim 10\text{ }\mu\text{m}$ below the surface was achieved in a total proton range of $\sim 20\text{ }\mu\text{m}$. Experiments lasted $\sim 90\text{ h}$, resulting in the calculated damage rate of 6.9×10^{-6} – 8.7×10^{-6} dpa/s. Dislocation loop, swelling, and grain boundary radiation induced segregation were studied by TEM. IASCC initiation was evaluated by constant extension rate test.

More details of the study is published in Journal of Nuclear Materials (J. Yang, et al., Journal of Nuclear Materials 560 (2022) 153493). A few more journal papers are in preparation.

This research was supported by the Laboratory-Directed Research & Development (LDRD) program of Idaho National Laboratory and the U.S. Department of Energy (DOE) Nuclear Science User Facilities (NSUF) experiment under DOE Idaho Operations Office Contract DE-AC07-05ID14517.



Grain structure, IASCC initiation, swelling and dislocation loops from different regions across a compositionally graded tensile specimens

DEFECT GENERATION AND PHASE STABILITY IN SINGLE CRYSTAL MIXED URANIUM-THORIUM OXIDES

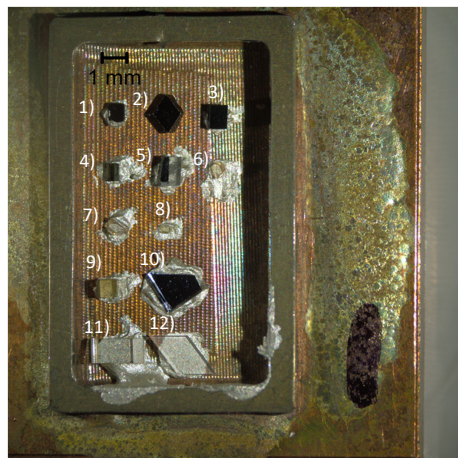
C.A. Dennett¹, M. Bachhav¹

¹Idaho National Laboratory

Mixed actinides of uranium-thorium dioxide have been considered for advanced fuel applications; alloying traditional UO_2 fuel with thorium in hope of imparting some of the increased thermal conductivity, higher melting point, chemical stability, and proposed proliferation resistance observed in ThO_2 . While fundamental data on unit phonon scattering mechanisms in either UO_2 or ThO_2 is still relatively scarce, no data presently exists for the $(\text{U,Th})\text{O}_2$ system with high (or equal) concentrations of both actinides. Importantly, a low-temperature miscibility gap has been computationally identified in these systems. However, given the extremely low native mobility of uranium and thorium metal cations, due in part to the fixed 4^+ oxidation state of Th, this miscibility gap is kinetically restricted in the few materials which have been synthesized in the relevant compositional range. Increased cation mobility under irradiation exposure may result in the observation of the proposed exsolution of UO_2 and ThO_2 domains (on the nanoscale), which will affect the thermal performance of the initially homogeneous solid solution microstructure.

In this work, a series of mixed oxides of $(\text{U,Th})\text{O}_2$ were irradiated with 2 MeV H^+ ions at 600°C to study both defect formation and microstructure stability, with some of the sampled chemistries inside the proposed miscibility gap at that temperature. Single crystals of multiple chemistries produced through hydrothermal synthesis were mounted to a custom, angled Cu plate to ensure no ion channeling effects during high temperature exposure under a raster scanned beam. Three fluences equivalent to 0.005, 0.05, and 0.5 dpa in the pre-peak plateau region targeted on identical sample matrices. The figure shows the as-mounted sample matrix containing $(\text{U,Th})\text{O}_2$ and several additional samples exposed to these conditions. At the time of this reporting, initial irradiation exposure has just been completed and no post irradiation analysis has yet taken place.

This work was supported by the U.S. Department of Energy, Office of Nuclear Energy under DOE Idaho Operations Office Contract DE-AC07-051D14517 as part of a Nuclear Science User Facilities experiment, and the Center for Thermal Energy Transport under Irradiation (TETI), an Energy Frontier Research Center funded by the US Department of Energy, Office of Science, Office of Basic Energy Sciences.



Sample ID	Notes
1) ThO ₂ -T-7b	50%U, 50%Th
2) ThO ₂ -T-9b	75%U, 25%Th
3) UO ₂ -T-355b	Zr:UO ₂
4) UThO ₂ -T-28b	UThO ₂ /ThO ₂ interface
5) UO ₂ -T-154b	UO ₂ /ThO ₂ interface
6) CeO ₂ -F-4b	CeO ₂ (111)
7) CeO ₂ -F-4h	CeO ₂ (111)
8) CeO ₂ -F-5b	Nd:CeO ₂ (111)
9) GaN-A-18b	GaN c-plane
10) GaAs-(111)-1b	GaAs (111)
11) SiC-VT-1b	SiC 6H, c-plane
12) Ga ₂ O ₃ -EF-1b	Ga ₂ O ₃ (010)

Optical image of as-prepared sample mounts for 2 MeV H^+ irradiation. Each sample matrix is fixtured to a single angled mounting plate (the sample pocket is machined with an 8° angle) such that raster-scanned proton irradiation can simultaneously exposure all single crystals to the same fluence and avoid any ion channeling effects. Three such fixtures were prepared for three exposures at 600°C as well as three identical spare fixtures as back-ups and should beam time be available for further exposure.

INVESTIGATION OF IRRADIATION-ASSISTED STRESS CORROSION CRACKING OF ADDITIVELY MANUFACTURED AUSTENITIC STAINLESS STEEL

J.-K. Lee¹, M. Ickes², O. Toader³, Zhijie Jiao³

¹ Department of Mechanical Engineering and Materials Science, University of Pittsburgh

² Westinghouse Electric Company

³ Department of Nuclear Engineering & Radiological Sciences, University of Michigan

The goal of this study is to develop the basic understanding of irradiation-assisted stress corrosion cracking (IASCC) in additively manufactured materials. The selected material system is Type 316 austenitic stainless steel which is widely used in parts of nuclear power plant and exhibits IASCC during power plant operation. The design freedom and potential ease of manufacture offered by additive manufacturing (AM) makes this process attractive to reactor engineers, and the implementation of additively manufactured components in nuclear reactors is being pursued by multiple commercial vendors.

To accomplish this objective, six slow strain rate test (SSRT) samples were irradiated to 5 dpa using the Michigan Ion Beam Laboratory. These samples included material produced by traditional extrusion and machining, laser powder bed fusion (LPBF), and binder jet printing (BJP). SSRT was then performed at the Irradiated Materials Test Laboratory at the University of Michigan. SSRT was carried out at 340°C in argon and in simulated PWR water. The results show that the mechanical properties of AM materials clearly depend on the processing technique, but ISCC was not clearly observed.

The samples also underwent post-irradiation examination (PIE) at Westinghouse Churchill Site and the University of Pittsburgh. At present scanning electron microscopy (SEM) preliminary examinations of the cracking induced by the testing has been completed, and further characterization including the use of focused ion beam (FIB) to view the cracks in cross-section is planned. All irradiated materials cracked when they were strained to 4% in both Ar and PWR water. Binder jet material had most cracking while wrought material had the least. Differences in cracking behavior are observable, for example by comparing fine-scale cracking observed in irradiated LPBF material strained in PWR water (**Error! Reference source not found.**) to irradiated wrought material strained in PWR water (**Error! Reference source not found.**), where cracks on the order of grain boundary lengths are visible.

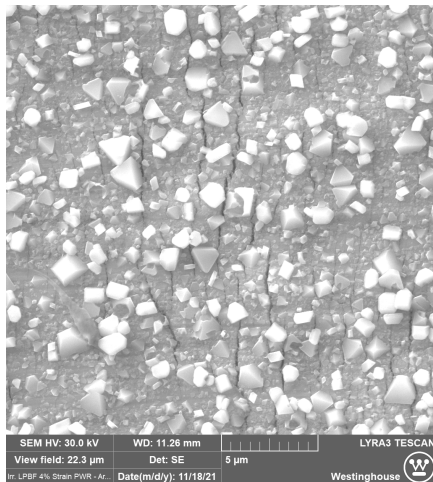


Figure 1. Fine cracking in LPBF material proton irradiated to 5 dpa and pulled to 4% strain in simulated PWR water.

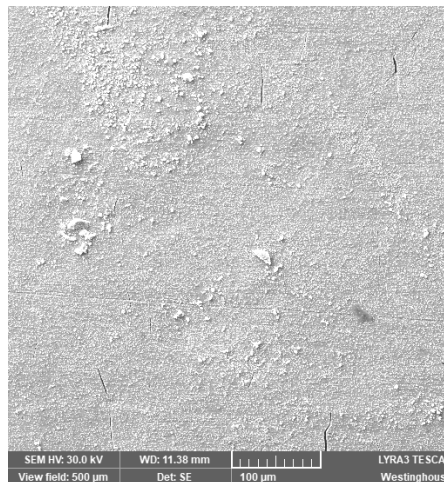


Figure 2. Cracking at grain boundary scale in wrought material proton irradiated to 5 dpa and pulled to 4% strain in simulated PWR water.

IRRADIATION PARAMETERS AND SINK STRENGTH DEPENDENCE OF RADIATION RESPONSES IN ADDITIVELY MANUFACTURED HT9 FERRITIC-MARTENSITIC STEELS

P. Xiu¹, N. Sridharan², K.G. Field¹

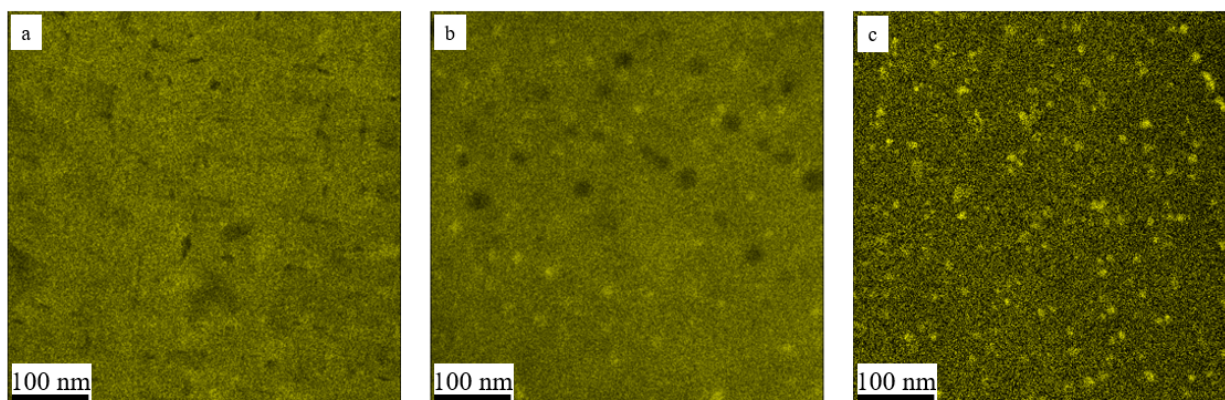
¹Department of Nuclear Engineering & Radiological Sciences, University of Michigan

²Lincoln Electric-India, India

The ferritic-martensitic (FM) steel HT9 is a promising candidate material for fast-fission reactor applications due to its superior swelling resistance. Radiation induced microstructural changes in HT9 including dislocation loops, precipitates, and cavities contribute to mechanical property degradation during the in-reactor service. Recently, the powder-blown laser directed energy deposition (DED), an additive manufacturing technique, coupled with post-build heat-treatments, was used to successfully fabricate HT9 alloys with flexible control over geometries and compositions (AM-HT9) [1–3]. The as-built (ASB) and the heat-treated conditions of AM-HT9 have drastically different starting microstructures and sink strengths, which is expected to significantly impact their radiation responses.

In this study, after AM-HT9 samples were produced using powder-blown laser DED at Oak Ridge National Laboratory's Manufacturing Demonstration Facility (MDF), two heat-treatment routes identical to those used for fabrication of wrought HT9, called ACO3 and FCRD, were used to decrease dislocation density, coarsen prior-austenite and lath grains, and form carbides. The three samples were dual ion-beam irradiated at the Michigan Ion Beam Laboratory (MIBL) to a total damage dose of 16, 50, 75, 100, 150, and 250 displacements per atom (dpa) with 4 He appm/dpa at 445°C. The STEM-EDX images in Figure 1 show the Ni-rich precipitates formation in the three conditions of AM-HT9. As shown, significant Ni clustering is observed in ACO3 and FCRD, both of which are heat-treated with lower sink strengths. On the contrary, Ni clustering is much less noticeable in the ASB specimen that contains much higher sink strength. A similar observation for the cavity evolution was made, where significant swelling and cavity growth occurred in ACO3 and FCRD whereas only minor swelling occurred in ASB specimen. The dislocation loop population remained mostly stable, because saturation was achieved in these alloys at much lower damage level of <20 dpa. Results indicate that the AM fabrication process and post-built heat-treatments have significant impact on the microstructural evolution and radiation responses in the HT9 alloys.

A portion of the irradiations were supported by the U.S. Department of Energy, Office of Nuclear Energy (DOE-NE), through Nuclear Science User Facilities project 18-1491. Preliminary characterization was supported by the Advanced Fuels Campaign - Nuclear Technology Research and Development program by the US Department of Energy, Office of Nuclear Energy under sub- contract 4000175183 through Oak Ridge National Laboratory



STEM-EDX images showing Ni-rich precipitation formation in (a) ASB, (b) ACO3 and (c) FCRD after dual beam irradiation to 250 dpa with 4 He appm/dpa at 445°C.

SYNERGISTIC PROTON IRRADIATION/CORROSION TESTS ON CVD SiC USED AS PROTECTIVE COATING OF SiC/SiC COMPOSITE ATF CLADDING MATERIALS

K. Lambrinou¹, B.T. Clay¹, R.D. Hanbury², K. Sun², J.A. Silverstein³, K.H. Yano³, S.L. Riechers³,
D.M. Frazer⁴, P. Xu⁴, E.J. Lahoda⁵, C.P. Deck⁶, R.L. Oelrich³, G.S. Was²

¹ School of Computing & Engineering, University of Huddersfield, Huddersfield, UK

² Department of Nuclear Engineering and Radiological Sciences University of Michigan

³ Pacific Northwest National Lab (PNNL), Richland, WA

⁴ Idaho National Lab (INL), Idaho Falls, ID

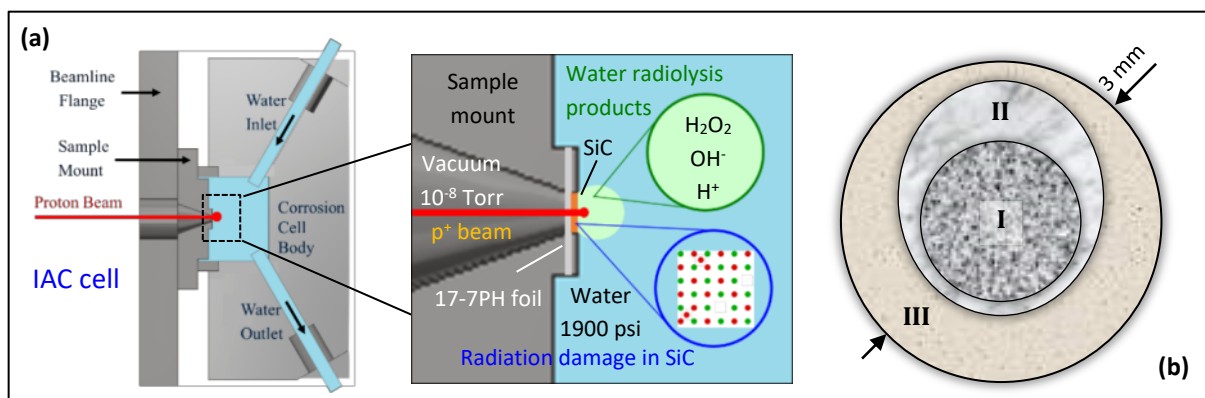
⁵ Westinghouse Electric Company LLC, Pittsburgh, PA

⁶ General Atomics (GA), San Diego, CA

Chemically Vapor Deposited (CVD) β -SiC has been proposed as coating material for SiC/SiC composite accident-tolerant fuel (ATF) claddings intended for use in Gen-II/III light water reactors (LWRs); these CVD SiC coatings, typically used as outer protection of CVI-infiltrated SiC/SiC composite fuel claddings, aim at reducing material losses under nominal operation conditions (i.e., in water of strictly controlled chemistry). SiC losses in water are attributed to the formation and subsequent dissolution of silica (SiO_2) (and other water-soluble Si species); however, little is known on the degradation mechanisms that operate in CVD SiC that is subjected simultaneously to irradiation and contact with different water chemistries.

In this work, three synergistic proton irradiation/corrosion tests were performed to study the degradation behavior of CVD SiC of industrial relevance (material supplied by GA). The tests were conducted in the unique irradiation-accelerated corrosion (IAC) cell (figure a) available at the Michigan Ion Beam Laboratory (MIBL) of the University of Michigan. The tested specimens were CVD SiC discs ($\varnothing 3 \pm 0.5$ mm, ~ 50 μm in thickness), while all irradiations were performed using a 5.4 MeV proton (p^+) beam at the following test conditions: (i) 320°C, standard PWR water with 3 ppm H_2 , (ii) 320°C, PWR water with 0.1 ppm H_2 , and (iii) 288°C, BWR water with 2 ppm O_2 and added H_2SO_4 to control the conductivity at 0.15 $\mu\text{S}/\text{cm}$. In all cases, the test duration was 48 h, which resulted in a displacement damage of 0.1 dpa (full-cascade SRIM calculations). The test configuration resulted in the formation of three distinct areas on the water-exposed facets of the SiC discs; the SiC degradation mechanisms in these areas were: (I) proton irradiation & water radiolysis, (II) water radiolysis, and (III) aqueous corrosion (figure b). The samples were studied before and after testing by SEM/EDS, AFM, FIB, TEM/STEM/EELS, ToF-SIMS, and micropillar compression.

This work was financially supported by (a) the U.S. Department of Energy, Office of Nuclear Energy under DOE Idaho Operations Office Contract DE-AC07-051D14517 as part of a Nuclear Science User Facilities experiment, and (b) the EURATOM research and training programme 2014–2018 under Grant Agreement No. 740415 (H2020 IL TROVATORE).



The IAC cell used for the synergistic proton irradiation/corrosion testing of CVD SiC (a). Area-specific degradation mechanisms: (I) proton irradiation & water radiolysis, (II) water radiolysis, and (III) aqueous corrosion (b).

Non-NSUF Projects

EFFECT OF CHROMIUM AND HELIUM ON CAVITY SWELLING IN DUAL-ION IRRADIATED HIGH PURITY IRON-CHROMIUM ALLOYS

Y. Lin¹, A. Bhattacharya², S.J. Zinkle^{1,2}

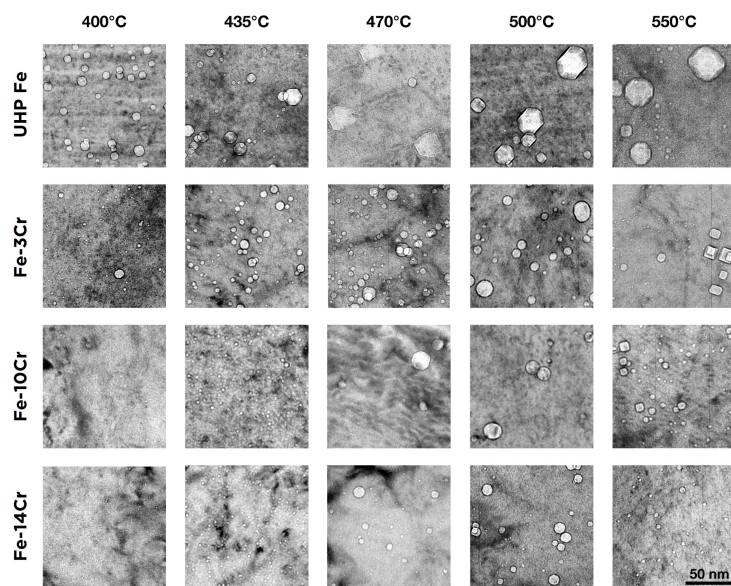
¹Department of Materials Science and Engineering, University of Tennessee

²Materials Science and Technology Division, Oak Ridge National Laboratory

Although research on temperature, radiation damage, and transmutant gas atom (He and H, especially) effects in reduced activation ferritic martensitic (RAFM) steels has spanned more than half a century, the knowledge of their irradiated properties is still far from complete. The complication is strongly influenced by their highly non-monotonic cavity-swelling and mechanical behavior as a function of the Cr concentration under irradiation. Also, the fluctuations of temperature or dose in neutron or reactor irradiation systems could affect the formation and evolution of defects. Thus, ion irradiation studies (with better temperature and dose control) on high purity Fe-Cr model alloys are needed to better understand the fundamental effects of irradiation in separate effects with limited variables.

This task aims to study the He synergistic effect on cavity swelling in ion-irradiated high purity Fe and Fe-Cr alloys. Simultaneous dual-beam irradiations on ultra-high purity Fe and Fe-Cr alloys (3-14 wt% Cr) at 400-550°C were performed to improve the understanding of cavity formation in ferritic alloys. 8 MeV Ni ions (relatively wide safe analysis zone with a midrange dose ~30 dpa) and helium production rates of 0.1-50 appm He/dpa were selected. He production rates of 10 and 50 appm He/dpa was selected to compare with our previous study on the same materials but irradiated at 0.1 appm He/dpa. Cavities were observed by TEM in all of the 0.1-50 appm He/dpa irradiated samples. A bimodal cavity size distribution was observed in samples with higher He production rate conditions. The peak swelling temperature was noticeably higher for the Fe-Cr alloys compared to pure Fe. Compared to the 0.1 He appm/dpa samples reported previously, the 10 appm He/dpa results showed a more considerable cavity swelling and higher peak swelling temperature.

This research was sponsored by the Office of Fusion Energy Sciences, U.S. Department of Energy under contract DE-AC05-00OR22725 with UT-Battelle, LLC (AB and SJZ) and grant # DE-SC0006661 with the University of Tennessee (YRL and SJZ).



TEM images of cavities in high purity Fe-Cr alloys irradiated by 8 MeV Ni and 3.55 MeV He ions at 400-550°C with 10 appm He/dpa. Data was carefully selected to avoid both surface effects and injected interstitial effects. Data were extracted from the 500 to 1250 nm range of the samples.

PROTON IRRADIATION AND LOW DOSE HEAVY ION IRRADIATION ON MODEL Fe-Cr AND Fe-Cu ALLOYS

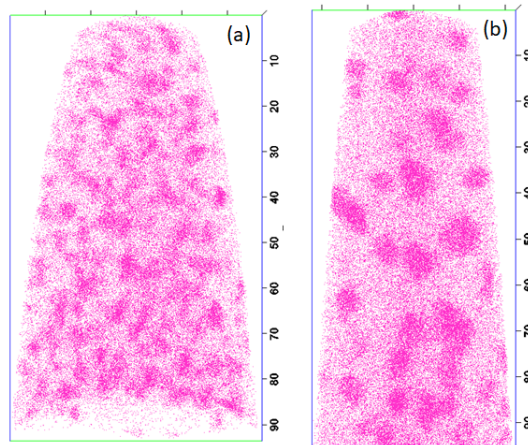
Y. Zhao¹, A. Bhattacharya², S.J. Zinkle^{1,2,3}

¹Material Science and Engineering Department, University of Tennessee, Knoxville

²Materials Science and Technology Division, Oak Ridge National Laboratory, Oak Ridge, TN

³Nuclear Engineering Department, University of Tennessee, Knoxville

Binary Fe-Cr alloys are simple representatives of ferritic-martensitic steels which are structural material candidates for Gen. IV fission and fusion reactors. One of the main barriers that impedes the understanding of this alloy system is the lack of a precise phase diagram at the low temperature regime, due to the slow diffusion rate of Cr atoms in Fe-enriched matrix. In order to accelerate the diffusion process and achieve steady states in a shorter time, Fe-(6-18)%Cr alloys were irradiated using 800 keV protons at temperatures of 250-450 °C to final doses of 2 dpa. The Cr-enriched alpha prime (α') precipitate distributions after irradiations were characterized using Atom Probe Tomography (APT) technique. The phase boundary will be deduced from the presence/absence of α' in alloys containing different Cr contents. Preliminary reconstructions have revealed the formation of α' after irradiation at 350 and 450 °C, and the Cr-atom maps are presented in the figure.



Reconstructions showing the formation of α' precipitates in Fe-18Cr after proton irradiation at 350 and 450 °C.

Heavy ion irradiations are capable of destroying pre-existing precipitates by producing displacement cascades. However, whether single displacement cascade can destroy the precipitates or not has been a question to both experimentalists and researchers working on simulations. In order to answer this question and to get a better understanding on how the size, crystal structure and composition of precipitates affect the dissolution process, ion irradiation to 0.1 dpa using 8 MeV Fe ions was performed on a series of model FeCr and FeCu alloys aged for different time to produce Cr or Cu precipitates. The irradiation temperature was set to -150 °C to suppress the back diffusion process. The characterization of as-aged and aged+irradiated specimens are in progress.

This work was supported by the Office of Fusion Energy Sciences, U.S. Department of Energy (grant # DESC000666 with the University of Tennessee and contract DE-AC05-00OR22725 with UT-Battelle, LLC).

HIGH FIDELITY ION BEAM SIMULATION OF HIGH DOSE NEUTRON IRRADIATION

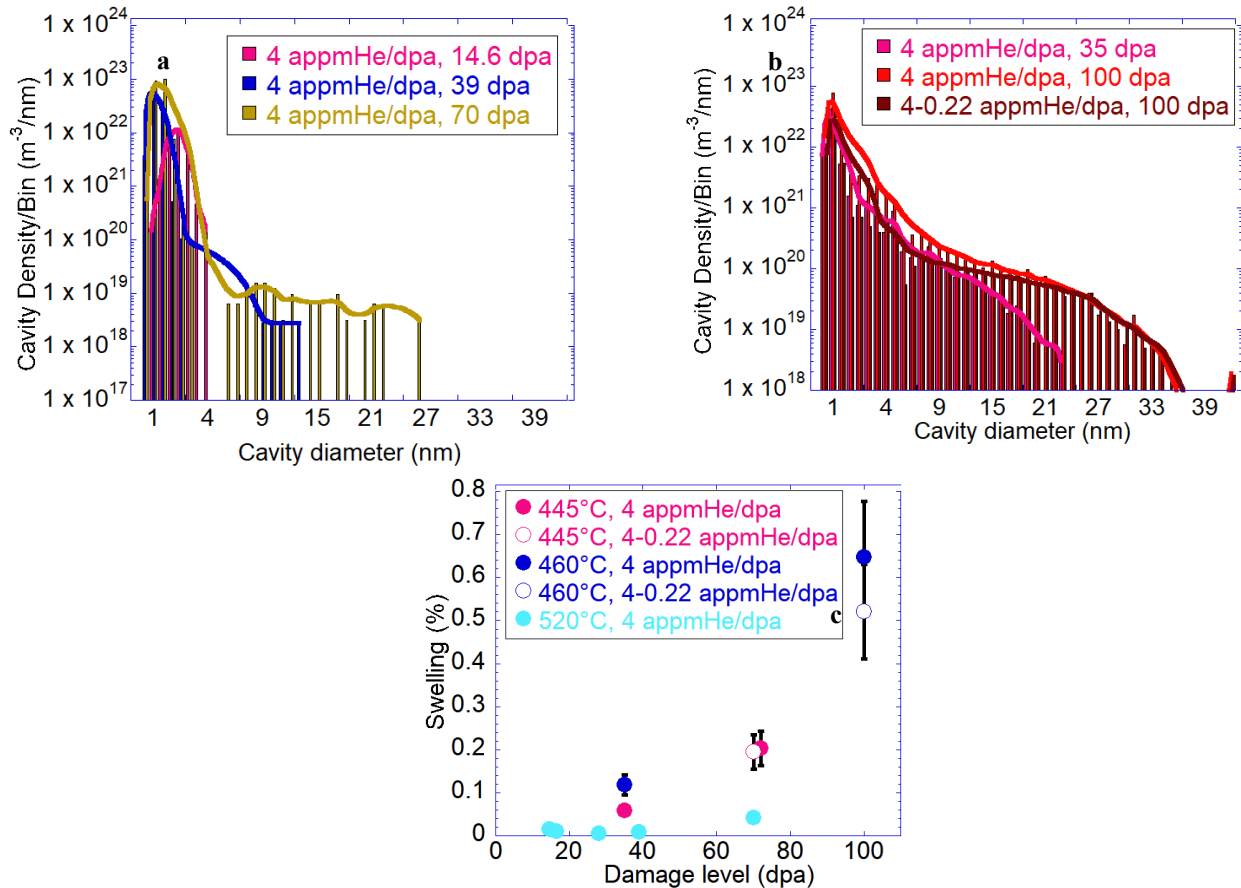
V. Pauly, S. Taller, Z. Jiao, K. G. Field, G.S. Was

Department of Nuclear Engineering & Radiological Sciences, University of Michigan

Traditional research efforts to understand radiation-induced processes in materials requires years of comprehensive post-irradiation characterization effort of test reactor produced neutron irradiated material. The same levels of radiation damage can be achieved using heavy ion irradiation under tightly controlled conditions in days or weeks instead of years in a nuclear reactor, albeit with several challenges because of the time compression. The purpose of this work is to address these challenges in using ion irradiation experiments as a surrogacy for neutron irradiation.

Several dual ion irradiations were performed using 9.0 MeV defocused Fe^{3+} ions to damage the material and simultaneously injecting He^{2+} ions to emulate gas buildup from nuclear transmutation reactions. Bars of T91 steel were dual ion irradiated up to 100 dpa with 4.3 appm He/dpa at 460 and 520 °C and to 100 dpa at 460 °C with 4.3 appm He/dpa for the first 35 dpa and 0.22 appm He/dpa for the remaining 65 dpa. These specimens are being examined with transmission electron microscopy to determine the effects of simultaneous helium injection and radiation damage on the irradiated microstructure of these materials.

This work is supported by the U.S. Department of Energy under award DE-NE0000639. This research was performed, in part, using instrumentation provided by the Department of Energy, Office of Nuclear Energy, Nuclear Technology R&D (formerly Fuel Cycle R&D) Program, and the Nuclear Science User Facilities.



Damage level and He injection level effect on (a) cavity size distributions at 520 °C, (b) cavity size distributions at 460 °C and (c) swelling.

SIMULATING NEUTRON IRRADIATION DAMAGE IN HT9 WITH HEAVY ION IRRADIATIONS

G. Bruno¹, K. Sun², K. G. Field¹

¹Department of Nuclear Engineering and Radiological Sciences, University of Michigan

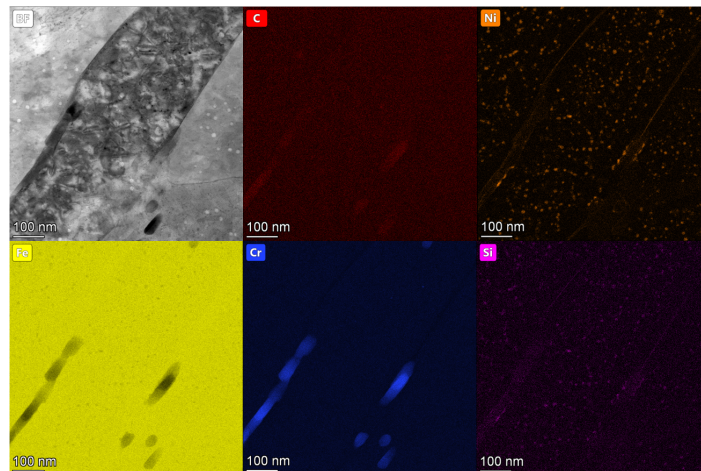
²Department of Materials Science and Engineering, University of Michigan

A ferritic-martensitic alloy, HT9, is under consideration as a structural material for advanced reactors. The testing of HT9 within materials test reactors takes several years to meet the appropriate damage levels characteristic of advanced reactor. Dual ion beams can be used to reach the desired damage levels in a significantly reduced time. By observing the microstructure of the heavy ion irradiated materials, an equivalent set of parameters can be found to emulate the microstructure of neutron irradiated materials from the BOR-60 fast reactor in Russia, which is the goal of these experiments.

Dual ion irradiations were run with 9 MeV Fe⁺⁺⁺ and 3.42 MeV He⁺⁺ to simulate damage as well as the production of helium within a typical nuclear reactor using a foil degrader to create the desired appm He per dpa profile during irradiation. The irradiation conditions range from 445°C to 570°C with damage levels as high as 80 dpa, and a 4.3 appm He per dpa ratio. Irradiations conducted this year included 2 at a dose rate of about 0.0001 dpa/s at 445°C to look at the formation of Cr-rich α' precipitation in the microstructure of HT9 at the typical dual ion irradiation conditions.

The samples are undergoing imaging at the Michigan Center for Materials Characterization at the University of Michigan - Ann Arbor for microstructural features that include cavities, dislocation loops, and radiation induced segregation. Cavities are imaged with scanning/transmission electron microscopy (S/TEM) techniques and dislocation loops are observed with on-zone STEM techniques [1]. STEM-EDS maps are taken with a Thermo Fisher Talos F200X G2 S/TEM. Figure 1 below shows a representative EDS map of Ni-Si clustering after a 54 dpa irradiation as well as cavities that formed as seen in the BF-STEM image.

Primary support for this research was provided by Department of Energy under contract DE-NE0000639.



Chromium and nickel-silicon clustering in HT9 irradiated at 445°C to 54 dpa.

HEAVY ION IRRADIATION OF Fe-15Cr MODEL ALLOY

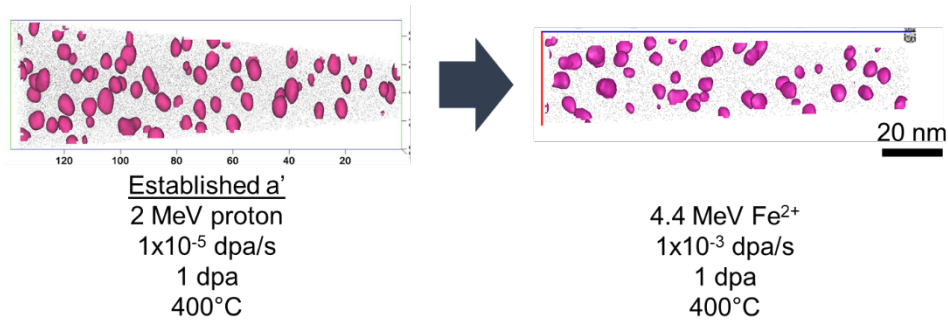
K.N. Thomas, Z. Jiao, G.S. Was

Department of Nuclear Engineering and Radiological Sciences, University of Michigan

High-chromium ferritic-martensitic (F-M) alloys are a candidate material type for future nuclear power plants due to the corrosion resistance and low swelling under irradiation. However, with chromium concentrations above ~9% and at lower temperatures below ~500°C, the F-M alloys are susceptible to the formation of the Cr-rich α' precipitates. Research has shown that the α' precipitates can be formed under thermal aging, as well as neutron, electron, and proton irradiation, but there is difficulty in the α' precipitate formation under heavy ion irradiation due to ballistic dissolution.

Model alloy Fe-15Cr was irradiated at the Michigan Ion Beam Laboratory (MIBL) in a series of experiments. The 15Cr samples had been previously irradiated at MIBL in 2019 with 2 MeV proton beam to 1 dpa at 400°C at 1×10^{-5} dpa/s to establish an α' precipitate microstructure. A previous irradiation experiment in 2020, further irradiated one of the proton irradiated samples with a 4.4 MeV Fe^{2+} raster-scanned beam at 1×10^{-4} dpa/s to 1 and 10 dpa. In 2021, an irradiation experiment repeating this experiment was completed except using an as-received Fe-15Cr sample in place of the proton irradiated sample. This experiment was motivated to confirm long-term stability of the α' precipitates under heavy ion irradiation at 1×10^{-4} dpa/s. APT results showed α' formation, thus confirming α' is stable under these irradiation conditions. An additional irradiation was completed in 2021 irradiating a proton irradiated sample further with 4.4 MeV Fe^{2+} raster-scanned beam at a damage rate of 1×10^{-3} dpa/s to 1 at 400°C. APT results showed ballistic dissolution of the α' precipitates with reduction in size and Cr concentration.

This work is supported by the U.S. Department of Energy under award DE-NE0000639.



APT reconstructions showing the α' distribution using an iso-concentration surface (35%Cr). The black dots represent 0.5% of the total Fe atoms in the volume.

ROLE OF MC AND $M_{23}C_6$ PRECIPITATES IN RADIATION RESISTANCE AND HELIUM DISTRIBUTION IN CASTABLE NANOSTRUCTURED ALLOYS

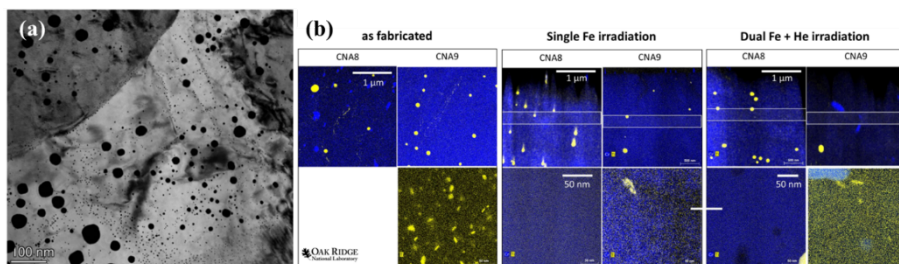
T. Graening¹, W. Zhong¹, L. Tan¹, P. Patki², K.G. Field²

¹MSTD, Oak Ridge National Laboratory, Oak Ridge, TN

²University of Michigan, Ann Arbor, MI

Bubble formation and growth can cause tens of percentage change in volumetric swelling in steels used in fusion reactors, creating a challenge for designing components that can accommodate this high swelling during service. Also, accumulation of helium to continuous microstructural features such as grain boundaries can embrittle a component leading to increased embrittlement in service. Ferritic-martensitic (FM) steels, including the subset of fusion-specific steels deemed reduced activation ferritic martensitic (RAFM) steels, have been developed to increase the density of dislocations, lath boundaries, solute additions, and precipitates to combat the effects of helium accumulation in high-creep strength steels. These microstructural features act as benign trapping sites for helium due to their discontinuous nature in FM and RAFM steel's microstructure. In the US, a new class of RAFM steel where composition and thermomechanical processing are used to increase helium trapping sites is under development. This class of steel, Castable Nanostructured Alloys (CNAs), have shown strong performance in preliminary laboratory-scale heat screening activities. Conventional RAFM steels, and CNAs, all rely on Cr solute additions and MX (M=metal, X=C/N) and $M_{23}C_6$ precipitates to resist helium-induced swelling. However, the role of MX and $M_{23}C_6$ precipitates in the presence of helium and radiation damage is not well understood as it may affect the precipitates stability as well. Hence, it is essential to probe the mechanisms associated with MX and $M_{23}C_6$ precipitates in helium tapping to refine the material's design for better high-dose radiation performance. Thus, single-beam and dual-beam ion irradiation experiments allow us to streamline the process of studying irradiation effects on the MX and $M_{23}C_6$ precipitates with and without helium co-injection in CNA alloys.

In this project, both single-beam and dual-beam irradiations using 9 MeV Fe^{3+} and 3.42 MeV He^{2+} were done at a temperature of 500°C at a dose rate of 7×10^{-4} dpa/s to a total dose of 50 dpa and 100 dpa, and for dual-beam irradiations the He^{2+} ions were co-injected at 10 appm/dpa. Hence, we would be able to emulate the effects of helium swelling in the material using dual-beam ion irradiation and discern the impact of helium co-injection on the stability of precipitates by comparing the single-beam and dual-beam irradiations. Preliminary results show that the dislocation loop population in the CNAs is suppressed due to the high irradiation temperature. At higher doses in both alloy, number density of voids increases 10 times from 50 dpa to 100 dpa. The lower carbon content CNA alloy does exhibit small MX precipitates (<5-10 nm) at high doses unlike the higher carbon content CNA alloy. Larger MX precipitates show stability under the irradiating conditions in both variants. This response is summarized in the figure. Further research is ongoing with respect to the precipitate stability at lower doses.



(a) Void distribution after dual beam irradiation of CNA9, (b) EDS maps showing precipitate stability after single/dual beam irradiation of MX precipitates in two CNA heats.

This work has been supported by the US Department of Energy (DOE), Office of Fusion Energy Sciences under the contract no. DE-AC05-00OR22725 with UT-Battelle, LLC and Early career award no. DE-SC0021138 with University of Michigan.

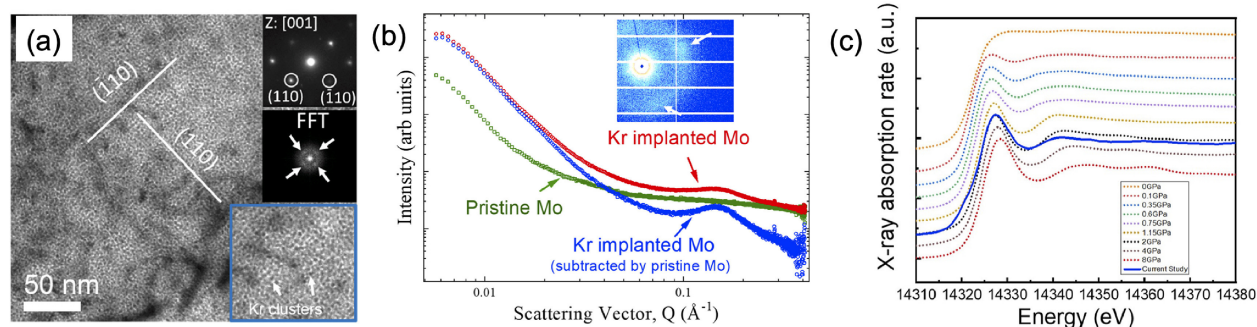
SELF-ORGANIZATION OF GAS BUBBLE SUPERLATTICE IN METALS AND ALLOYS UNDER ION IMPLANTATION

C. Sun and J. Gan
Idaho National Laboratory, Idaho Falls, ID 83415

Self-organization of defects in materials has significant scientific merit and great technological impact due to the creation of novel physical properties with potential applications in various industries. In nuclear fuels, the formation of ordered defect superlattices could effectively store the fission gas and prevent large structural distortions due to swelling, because ordered fission gas bubbles could prevent bubble interconnection that drives detrimental behaviors. Irradiation damage generates non-equilibrium ordered defect structures, such as gas bubble superlattice (GBS), void superlattice, and stacking fault tetrahedron alignments. Previously, we studied the formation mechanism of void superlattice and helium (He) gas bubble superlattice formation and constructed the formation window of void and He gas bubble superlattice in bcc Mo. As the inert gas atoms change from light ion species (e.g., He) to heavy ion species (e.g., Xe), the ordering of the gas bubbles becomes more challenging and formation mechanisms could be modified. The objective of this project is to compare the formation mechanisms of defect superlattices with various gas ion species and manage the evolution of defect superlattice in a controllable way. The success of this work will have a tremendous impact to the design of advanced nuclear fuels and precisely predict the fuel performance in nuclear reactors. This work is to support the U.S. Department of Energy's (DOE) Basic Energy Science (BES) core project at Idaho National Laboratory on "The Role of Anisotropy on Self-Organization of Gas Bubble Superlattice (GBS)".

In this work, systematic implantation experiments have been performed to develop formation window of gas bubble superlattice in fcc and bcc metals. Ni, Fe, Mo, and Cu. TEM discs have been irradiated with He, Kr, and Xe ions at different fluences and temperatures using the 400 keV ion implanter at MIBL. The fixture shows an example of Kr bubble superlattice in Mo under irradiation at 400°C. Irradiation of W-Re alloys and U-Mo alloys are still on the way. Two-step irradiation experiments (low energy ion implantation followed by high energy ion irradiation) will be performed as well. Two-step irradiation involves low energy ion implantation to form GBS and followed by high energy 1.2 MeV Xe ions (Xe³⁺) to add additional damage in displacements-per-atom (dpa) without significantly altering the gas content in GBS region.

This work is sponsored by the U.S. Department of Energy (DOE) Office of Science, Basic Energy & Science, Materials Sciences and Engineering Division under FWP #C000-14-003 at Idaho National Laboratory, operated by Battelle Energy Alliance under contract DE-AC07-05ID14517.



Formation of solid bubble superlattice in Mo under Kr ion implantation at 400°C to a fluence of $2.5 \times 10^{16} \text{ cm}^{-2}$. (a) TEM micrograph showing Kr bubble superlattice. (b) Small-angle X-ray scattering measurement of Kr bubble superlattice in Mo. (c) X-ray near edge structure measurement of inner pressure of solid Kr bubbles.

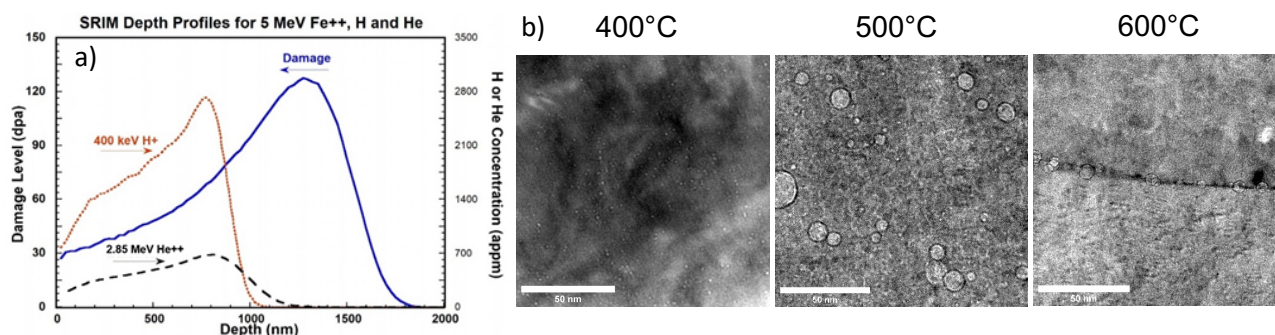
Response of Candidate Fusion Blanket Materials to Dual and Triple Ion Irradiation to Understand the Synergies between H, He and Radiation Damage

L. N. Clowers¹, Z. Jiao¹, F. Naab¹, P. Niraula¹, G.S. Was¹

¹ Department of Nuclear Engineering & Radiological Sciences, University of Michigan

The goal of this study is to investigate the nucleation and growth of cavities and bubbles using multiple ion beams to capture the production of gasses by transmutation in ferritic alloys for fusion blanket materials. The role of H in the nucleation and growth of He bubbles into cavities remains largely unanswered and poorly understood and is critical to assessing performance of candidate alloys for a fusion blanket and first-wall environment. Such behavior will affect the evolution of the irradiated microstructure and could accelerate processes such as He bubble nucleation, transformation of bubbles to cavities and even cavity growth. To investigate these phenomena, a series of irradiations was conducted on three reduced activation ferritic/martensitic (RAFM) steels; F82H (IEA heat from the National Institutes of Quantum and Radiological Science and Technology in Japan), CNA3 (from ORNL) and Fe8Cr2W (made at Ames laboratory). Ion irradiations were conducted using the 3 MV Pelletron accelerator to provide a defocused beam of 5 MeV Fe²⁺ for irradiation damage, the 1.7 MV Tandetron to provide a raster-scanned beam of 2.85 MeV He²⁺ to be passed through a ~6.4 μm thick Al degrader foil for helium implantation, and the implanter to provide a raster-scanned beam of 390 keV H⁺ through a second ~2.3 μm Al degrader foil for hydrogen implantation. Samples were irradiated in the multi-beam chamber (MBC). Three types of ion irradiation, single ion beam (Fe²⁺), dual ion beam (Fe²⁺+He²⁺), and triple ion beam (Fe²⁺+He²⁺+H⁺) were conducted from 400°C to 600°C to a damage level of 50 dpa to investigate the temperature effects of these phenomena. The damage profiles from self-ions and the concentration profiles of injected H/He calculated using a custom Python script along with SRIM-2013 are shown in figure (a). The appm/dpa ratios for helium and hydrogen are 40 appm/dpa and 10 appm/dpa, respectively, at the depth of analysis (500-700nm from the surface). Helium reached 2000 appm and hydrogen reached 500 appm in the region of interest at the end of 50 dpa irradiation at a damage rate of ~1x10⁻³ dpa/s. Thermocouple measurements were used to calibrate the thermal imaging for the temperature determination and were recorded along with pressure and beam current during these irradiation experiments. Post-irradiation microstructural characterization was subsequently performed on focused ion beam (FIB) lift-outs of the irradiated materials via transmission electron microscopy at the Michigan Center for Materials Characterization (MC²). The cavity microstructure of F82H after triple ion irradiation is shown in figure (b) where the temperature dependence on void swelling in the triple ion irradiated material is quite apparent with a peak swelling temperature at around 500°C where co-injection of H⁺ was observed to cause a substantial increase in the void swelling of each alloy when compared to traditional dual ion irradiation.

This material is based upon work supported by the U.S. Department of Energy, Office of Science, Office of Fusion Energy Sciences under Award Number DE-SC0020226.



Displacement and implantation curves for 5 MeV Fe²⁺ and energy degraded He²⁺/H⁺ in F82H RAFM steel (left).
TEM-BF images of triple ion irradiated F82H at 400°C, 500°C, and 600°C (right)

RADIATION DEGRADATION OF A NOVEL POLYMER SCINTILLATOR

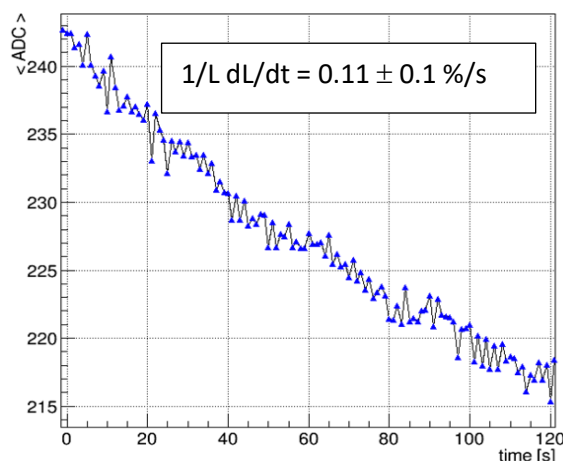
D. Levin¹, C. Ferretti¹, P. Friedman², A. Kaipainen¹, N. Ristow¹

¹University of Michigan, Randall Laboratory, 450 Church St, Ann Arbor, MI

²Integrated Sensors, LLC, 201 Thornton Drive, Palm Beach Gardens, Florida 33418

Our group is investigating the scintillation light output observed in a semi-crystalline polymer material (PM) as a function of ionizing radiation dose. PM is common organic thermoplastic with broad commercial and industrial usage. It is available in bulk and film form and is characterized by high tensile strength, dimensional stability, oxygen impermeability, low water absorption. When excited by ionizing radiation it has a blue light emission peak.

Of specific interest are novel applications of this material for use in ion beam instrumentation for research and for new cancer therapy modalities. Like all organic scintillators, radiation induced degradation in the form of light yield reduction is presumed to occur when ionized molecules of the solvent are damaged and can no longer emit visible light, and from formation of metastable radicals which can recombine to produce other species that act as light quenching agents.



This study was conducted at the Michigan Ion Beam Laboratory (MIBL) in September 2021. Previous studies of PM radiation damage were conducted on bulk material by measurement of the scintillation light before and after exposure. This work investigates specifically very thin ($< 200 \mu\text{m}$) PM films, and directly and continuously measures their light yield response during exposure to a heavily ionizing proton beam. The measurement was made using a sensitive machine vision camera using the digitized analogue to digital (ADC) signal output. Shown at left is the absolute light yield, measured in ADC counts, of a $3.0 \mu\text{m}$ PM film while being irradiated by a 1.0 MeV proton beam. The equivalent dose rate was $D_R = 136 \pm 24 \text{ Gy/s}$. The

fractional signal loss during a 2 minute irradiation time was $0.11 \pm 0.015 \text{ %/s}$ (see Figure), corresponding to relative light loss per dose of $S = 0.8\% \pm 0.1\%$ per kGy of absorbed radiation dose. The light loss is attributed to a combination of lower scintillation efficiency and to reduced light transmission through the medium. Deconvolving the relative contributions of these processes is the objective of ongoing work.

This work was funded by an SBIR Phase-II award from the DOE Office of Science to Integrated Sensors, LLC (Award No. DE-SC0019597). We are grateful for the kind assistance of the Michigan Ion Beam Laboratory staff. Results of this work are included in our submission to the PTCOG-60 conference, Miami, FL, June, 2022.

MICROSTRUCTURE, MECHANICAL PROPERTIES, AND IRRADIATION RESPONSE OF Fe-Cr-Ni-BASED MULTI-PRINCIPAL ELEMENT ALLOYS

M.E. Parry^{1,2}, W. Jiang³, C. Sun⁴, B. Kombaiah⁴, and T.D. Sparks²

¹ Irradiated Fuels & Materials Department, Idaho National Laboratory

² Department of Materials Science & Engineering, University of Utah

³ Computational Mechanics & Materials Department, Idaho National Laboratory

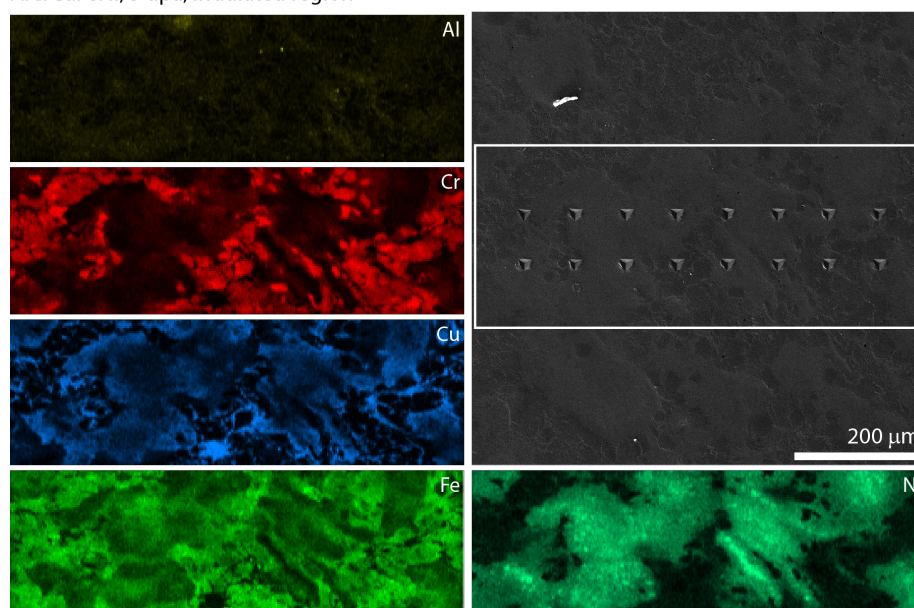
⁴ Advanced Characterization Department, Idaho National Laboratory

The implementation of advanced nuclear design concepts requires advanced structural materials to withstand the associated harsh conditions, including elevated temperatures, pressures, and radiation doses, while some designs also involve new coolant environments. Multi-principal element alloys (MPEAs) may address these challenges as they have demonstrated extraordinary strength, hardness, oxidation and corrosion resistance, thermal stability, and radiation tolerance, driving appeal as potential reactor structural materials. However, composition-microstructure-property relationships among MPEAs remain unclear, particularly relating to irradiation damage.

To clarify these relationships, four MPEAs in the Al-Cr-Fe-Ni-(Cu,Mn) system were selected, including: FeCrNiMnAl_{0.3}, FeCrNiCuAl_{0.3}, FeCrNiCuAl, and FeCrNiMnAl. The alloys were prepared to 2-mm×2-mm×20-mm dimensions through cryogenic milling of elemental powders, spark plasma sintering into bulk alloy ingots, electrical discharge machining, and surface polishing to a 3-μm finish. Using Michigan Ion Beam Laboratory facilities, the alloys were irradiated with 2.0 MeV protons at 400 °C to damage levels of 2, 3, and 5 displacements-per-atom. Examination of phase stability and nanomechanical response of pre- and post-irradiated specimens will elucidate correlations among alloy chemistry, microstructure, and irradiation damage tolerance in MPEAs.

This work was supported through the INL Laboratory Directed Research & Development (LDRD) Program under DOE Idaho Operations Office Contract DE-AC07-05ID14517.

AlCrCuFeNi, 5 dpa, irradiated region



Representative micrograph of the AlCrCuFeNi alloy proton irradiated to 5 dpa. A 2×8 nanoindentation grid is visible in the SEM image (upper right), and corresponding EDS maps are also illustrated. Results will clarify relationships among microstructure, mechanical response, and irradiation damage.

STUDY OF SURFACE BLISTERING FORMATION USING ION IMPLANTATION

X. Zhai, Z. Jian, E. Ahmadi and F. Naab

Department of Electrical Engineering and computer science, University of Michigan

The goal of this study is to use ion implantation to get surface blistering and finally achieve smart cut. Multiple ion implantation were tried in MIBL. The first implantation condition was done at 300°C with 90 keV helium 1.5×10^{17} i/cm² followed by 60 keV hydrogen 1.5×10^{17} i/cm². The result is not desirable. As shown in figure 1, some surface damage happens because of high implantation temperature. This type of surface damage cannot be used for low temperature bonding. Then a second implantation was done. The condition is room temperature with 90 keV He 1.5×10^{17} i/cm² followed by 60 keV H 1.5×10^{17} i/cm². Under this condition, surface damage didn't happen and the bonding was successful. As you can see in figure 2.

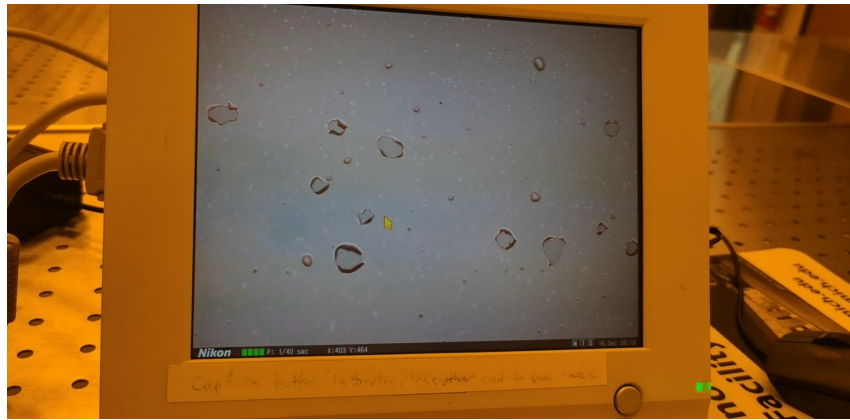


Figure 1. implantation of 90 keV He at 300°C to 1.5×10^{17} i/cm² followed by 60 keV hydrogen to 1.5×10^{17} i/cm².

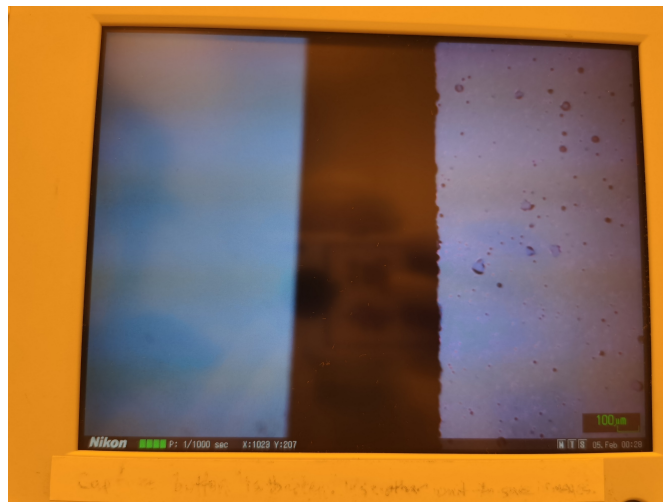


Figure 2. Implantation of 90 keV He at room temperature to 1.5×10^{17} i/cm² followed by 60 keV H 1.5×10^{17} i/cm².

DOPING OF RUTILE GERMANIUM OXIDE

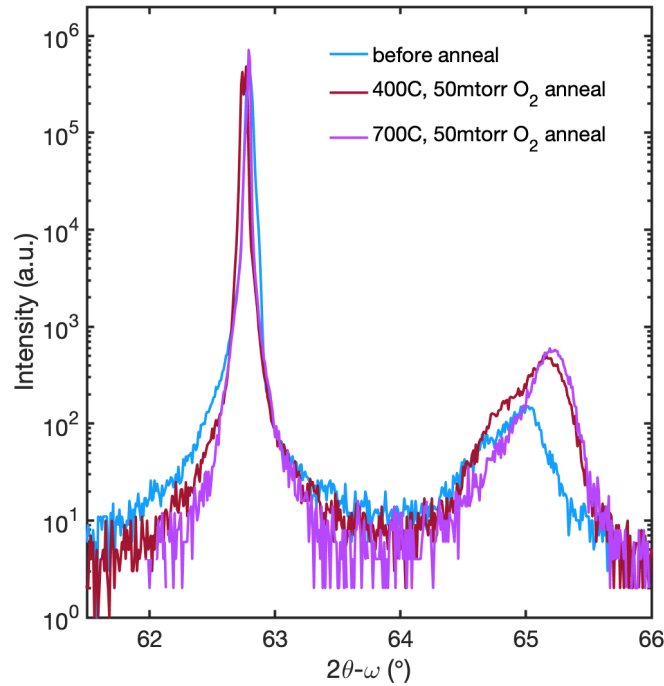
S. Chae¹, E. Kioupakis¹, J. Heron¹

¹Department of Materials Science Engineering, University of Michigan

Power electronics seek to improve power conversion of devices by utilizing materials with a wide-band-gap, high carrier mobility, and high thermal conductivity. Due to its wide-band-gap of 4.5 eV, β -Ga₂O₃ has received much attention for high-voltage electronic device research. Rutile GeO₂ (r-GeO₂) is a potential ultra-wide-band-gap (UWBG, 4.68 eV) semiconductor, yet is unexplored for electronic applications. Our first-principles calculations predict shallow ionization energies (<0.04 eV) for donors such as Sb_{Ge}, As_{Ge}, and F_O, and an ionization energy of 0.45 eV for Al_{Ge} acceptors, suggesting the possibility of ambipolar doping. Though the thin-film synthesis of r-GeO₂ has remained challenging due to the presence of highly metastable amorphous phase, we demonstrate the first synthesis of single crystalline thin films on r-GeO₂ on a sapphire substrate as well as a TiO₂ substrate using ozone-assisted molecular beam epitaxy. Our work motivates further exploration of doping of r-GeO₂ thin films by ion implantation to apply r-GeO₂ as an alternative UWBG semiconductor that can overcome the limitations of the current UWBG semiconductor materials.

r-GeO₂ thin films on TiO₂ substrates were irradiated with F⁻ ions at room temperature. The beam conditions of 50 keV energy and 1E+14 atoms/cm² were used. After implantation, we annealed the films at 400 °C and 700 °C to recover structural damages of the films. We then measured electrical conductivity of our films using Keithley 4200.

This work was supported by the National Science Foundation [Platform for the Accelerated Realization, Analysis, and Discovery of Interface Materials (PARADIM)] under Cooperative Agreement No. DMR-1539918.



X-ray diffraction patterns of F⁻-implanted r-GeO₂ films on (Ge,Ti)O₂-buffered TiO₂ 001 substrates before and after post-annealing.

STUDY OF THE RADIATION RESISTANCE OF Cr-Al-B MAB PHASES WITH COMPARISON TO Cr-B PHASES

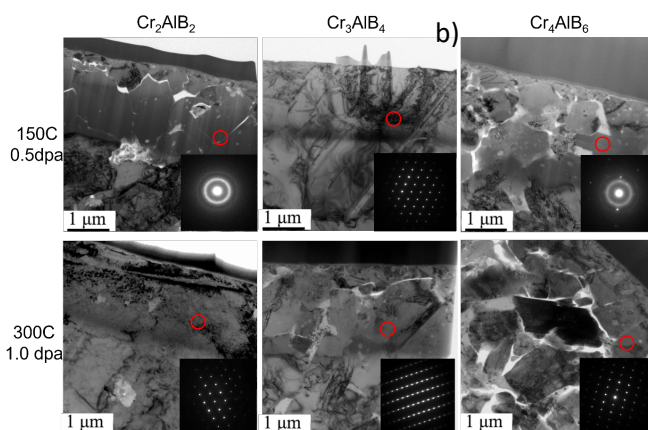
H. Zhang¹, J. Y. Kim¹, I. Szlufarska

Department of Material Science, University of Wisconsin-Madison

The goal of this study is to examine the radiation tolerance of the new series of layered ceramic material, the MAB phase. The layered ceramics have been shown to have many great properties, including thermal shock resistance, oxidation resistance, hardness, strength, and radiation resistance. Radiation effects have been studied primarily in MAX phases (M = early transition metal, A = group A element in the periodic table, and X = C or N), which in some cases can maintain their crystalline structures up to a very high radiation dose. However, the radiation-induced cracks and phase transformation limit the application of the MAX phase. MAB phases are a new class of layered ternary materials that have already shown a number of outstanding properties. While the radiation tolerance has never been studied.

Here, we investigate defect evolution and radiation tolerance of three MAB phases, Cr₂AlB₂, Cr₃AlB₄ and Cr₄AlB₆, using a combination of experimental characterization and first-principles calculations. To examine the radiation effects, the MAB phase materials, together with their corresponded binary Cr-B phases (CrB, Cr₂B₃ and Cr₃B₄), were irradiated at two different temperatures with 6.0 MeV Si-ion at the Michigan Ion Beam Laboratory. We find that Cr₃AlB₄ is the most tolerant to radiation-induced amorphization than other MAB phases, both at 150 °C and at 300 °C. The results can be explained by the fact that the Cr Frenkel pair is unstable in Cr₃AlB₄, and as a result, irradiated it is expected to have a significant concentration of Cr-Al antisites, which are difficult to anneal even at 300 °C. We find that the tolerance to radiation-induced amorphization of MAB phases is lower than in MAX phases, but it is comparable to that of SiC. However, MAB phases do not show radiation-induced cracking which is observed in MAX phases under the same irradiation conditions. This study suggests that MAB phases might be a promising class of materials for applications that involve radiation.

This work was supported by the U.S. Department of Energy, Office of Science, Basic Energy Sciences under Award # DE-FG02-08ER46493.



TEM images of Cr₂AlB₂, Cr₃AlB₄, and Cr₄AlB₆, irradiated at 1.3×10^{16} ions·cm⁻² at 150 °C (top row), at 2.6×10^{16} ions·cm⁻² at 300 °C (bottom row). The red circle in each image corresponds to the region that was analyzed by selected area diffraction (SAED).

IN SITU TEM STUDY OF EFFECTS OF HEAVY ION IRRADIATION IN HOLLANDITE COMPOSITIONS

L.M. Wang^{1,2}, K. Sun², Y. Li²

¹Department of Nuclear Engineering and Radiological Sciences, University of Michigan

²Department of Material Science and Engineering, University of Michigan

Hollandite with a general formula of $A_{1-2}(B,C)_8O_{16}$ is a promising family of crystalline ceramic materials proposed for using as the nuclear waste form to immobilize radioactive alkali and alkaline earth elements (e.g., Cs and Ba) in high-level waste (HLW)[1]. Previous study using electron beam irradiation to simulate the effects of β -decay of Cs-137 has demonstrated an excellent stability of the Ba/Cs-Fe/Ti series of hollandite. In this study, heavy ion irradiation is used to simulate the effects of β -decay of transuranic elements (TRU) to explore the feasibility of using hollandite as the waste form for TRU. *In situ* transmission TEM in the electron diffraction mode was carried out during 1.2 MeV Kr^{3+} irradiation at the room temperature using a 300 kV FEI Tecnai TEM that is interfaced with a 400 kV ion implanter at the Michigan Ion Beam Laboratory (MIBL). The progressive process of irradiation-induced solid-state amorphization of two hollandite compositions, i.e., $Ba_{1.33}Fe_{2.66}Ti_{5.34}O_{16}$ (Ba-end member) and $Cs_{1.33}Fe_{1.33}Ti_{6.67}O_{16}$ (Cs-end member) has been followed and analyzed (Figs. 1 and 2). Although both compositions fully amorphized after only a fraction of a dpa, the Cs-end member took $\sim 50\%$ extra dose to become fully amorphous indicating an advantage of using the hollandite as a dual-purpose waste form for both fission products (e.g., Cs and Ba) and TRU (e.g., Pu and Am).

This work is supported by the Center for Hierarchical Waste Form Materials (CHWM), an Energy Frontier Research Center funded by the U.S. Department of Energy.

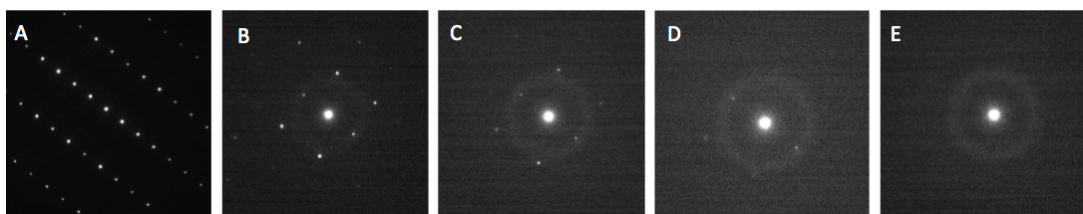


Figure 1. A series of selected area electron diffraction patterns showing the process of amorphization of $Ba_{1.33}Fe_{2.66}Ti_{5.34}O_{16}$ after (A) 0, (B) 0.1, (C) 0.14, (C) 0.18, and (D) 0.22 dpa.

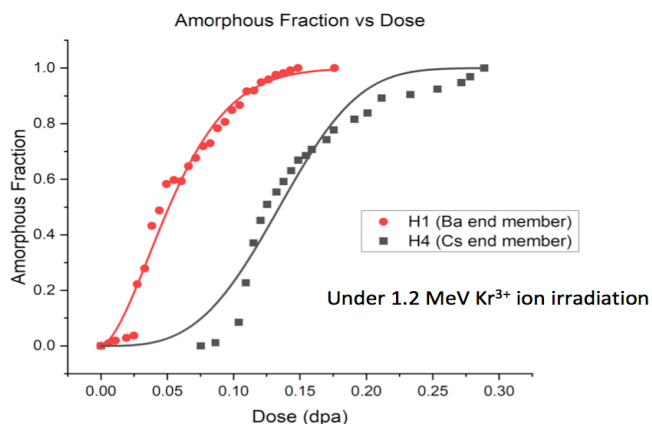


Figure 2. Amorphous fraction vs. dose curves for both B- and Cs-end members of hollandite compositions.

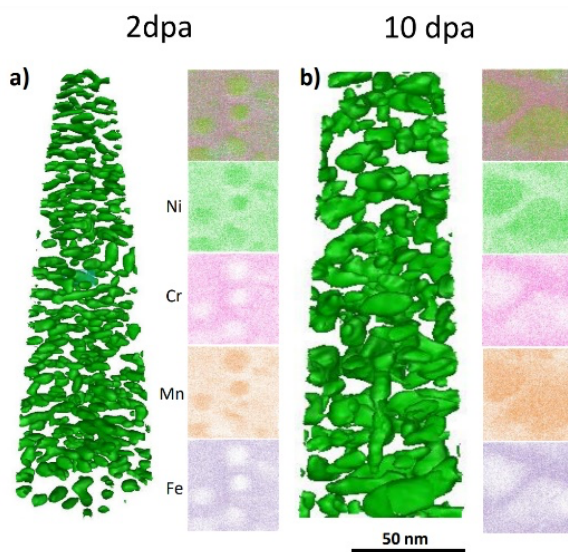
MECHANISMS CONTROLLING THE IRRADIATION RESPONSES OF CONCENTRATED MULTI-COMPONENT ALLOYS

Anshul Kamboj¹ and Emmanuelle Marquis¹

¹Department of Materials Science and Engineering, University of Michigan

The goal of this study is to examine the effects of composition and dose rate on the irradiation behavior of concentrated multi-component alloys. As we move from dilute to concentrated solid solution alloys, there is a change in the energy and mass transport properties of the material. To understand the impact on the alloys' radiation behavior, we studied a range of compositions within the Ni-Cr-Fe-Mn-Co system. The systematic variation in number and nature of elements as well as control of the irradiation conditions allowed us to study the effect of composition, dose, and dose rate.

For example, several CrFeNi-based MPEAs appeared stable against phase decomposition during high dose rate ion irradiation [1], however, electron irradiation and thermal annealing studies found that these alloys are susceptible to phase decomposition [2]. To verify that phase stability is a result of cascade mixing at high dose rate, we studied the irradiation behavior of these alloys using lower dose rate. The alloys used in the study were synthesized using arc melting and homogenized at 1200 °C. Alloys were irradiated using 6 MeV Fe³⁺ ions using Maize and Wolverine accelerator using a Cu stage heated to 500 °C. The target damage was 2 dpa and 10 dpa at 700 nm below the surface, achieved using 10⁻⁴ dpa/s and 10⁻⁵ dpa/s. Atom probe tomography and transmission electron microscopy characterization revealed phase decomposition and a high number density of Ni-Mn precipitates in Cr₁₈Fe₂₇Ni₂₈Mn₂₇ after ion irradiation at 10⁻⁴ dpa/s, as illustrated in the figure.



APT reconstruction highlighting the distribution of Ni-Mn rich precipitates after irradiation using a 75 at.% Ni+Mn iso-concentration surface and Ni, Cr, Mn, and Fe maps taken from 30x30x10 nm³ slice, revealing Ni-Mn rich precipitates (a) at 2 dpa, and (b) at 10 dpa.

INFLUENCE OF Mg/N CO-IMPLANTATION + GYROTRON ANNEALING ON ATOMIC DISPLACEMENTS IN GaN

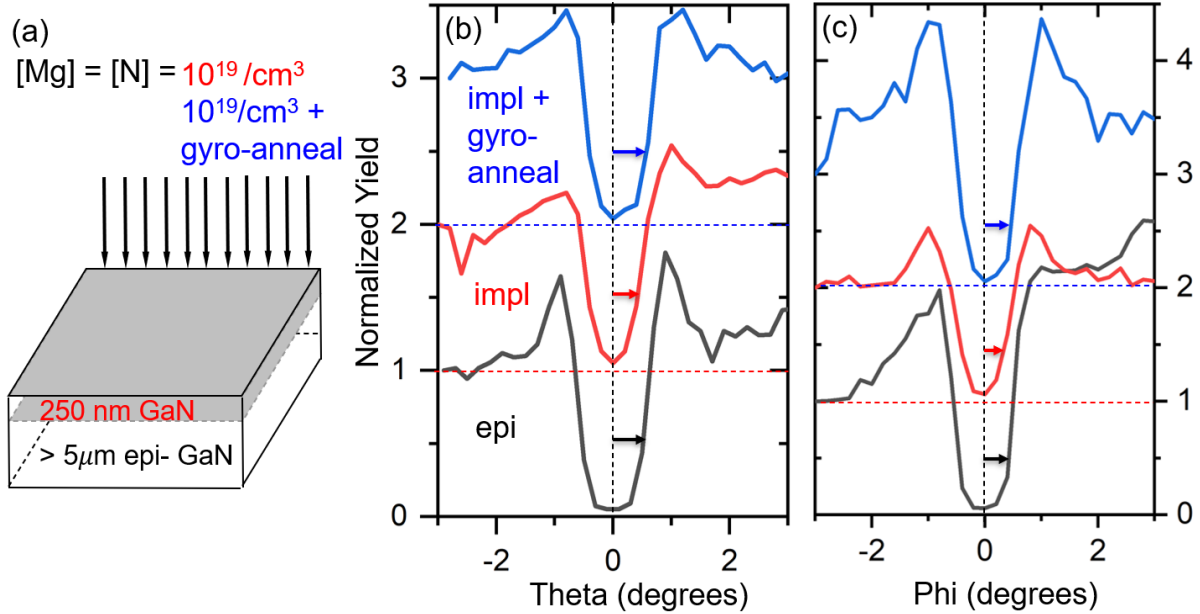
Z. Zhang¹, J. Cooper¹, F. Naab², R.S. Goldman¹, V. Meyers³, S. Shahedipour-Sandvik³

¹Department of Materials Science and Engineering, University of Michigan

²Department of Nuclear Engineering and Radiological Sciences, University of Michigan

³Nanoscale Science and Engineering, State University of New York (SUNY) - Albany

Wide bandgap semiconductors such as GaN play an increasingly important role in high-frequency, high-power, and high-temperature electronics. In the quest to achieve vertical p-n diodes for high power devices, several approaches to selected-area p-type doping of GaN have been explored. For example, p-type doping with minimal N vacancy formation has been achieved using Mg/N co-implantation followed by ultra-high pressure (UHP) annealing in a N₂ atmosphere, with or without microwave pulsing. To examine the influence of UHP annealing with microwave pulsing (“gyrotron annealing”) on atomic displacements in Ga/N co-implanted GaN, we have utilized channeling Rutherford Backscattering Spectroscopy (RBS/c) at MIBL. Epitaxial GaN was Mg/N co-implanted, each to 10¹⁹/cm³ within 250 nm depth, followed by five 8-second gyrotron pulses at 1450°C. RBS/c reveals that Mg/N co-implantation increases the minimum yield, χ_{\min} from 0.02 to 0.06, indicating that 4% of Ga atoms are displaced. Angular yield scans reveal a corresponding 0.11 Å displacement of Ga atoms into the channels. Following gyrotron annealing, χ_{\min} is reduced to 0.04, indicating that the fraction of displaced Ga has decreased to 2%. Angular yield scans reveal 0.08 Å displacement of Ga atoms, comparable to the thermal vibrational amplitude of 0.062 Å. The concentration of displaced Ga atoms, [Ga_{displaced}] ~ 10²¹/cm³, is likely due to the formation of V_{Ga} and Ga_i in addition to Mg_{Ga}.

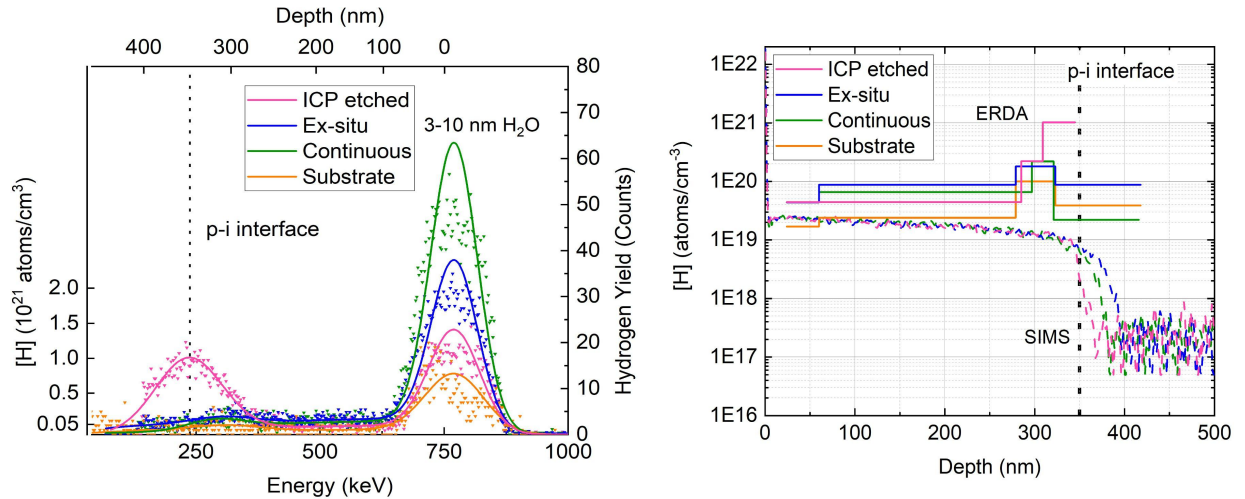


(a) Diagram of Mg/N co-implanted + gyrotron microwave annealed GaN structures. Angular yield scan profiles along (b) <110> and (c) <1120>. Mg/N co-implantation narrows the angular yields from 0.50° to 0.42°, suggesting that Ga atoms are displaced into channels by 0.11 Å. Subsequent gyrotron annealing widens those angular yields to 0.45°, reducing Ga atomic displacements to 0.08 Å, comparable to the thermal vibration amplitude.

QUANTIFYING H AT P-GaN/I-GaN INTERFACES USING ELASTIC RECOIL DETECTION ANALYSIS

J. Cooper, J. He, G. Cheng, Thales Borrelly dos Santos⁺, F. Naab^{*}, and R.S. Goldman
Materials Science & Engineering, ^{*}Michigan Ion Beam Laboratory
University of Michigan, Ann Arbor MI; ⁺Physics Institute, University of Sao Paulo, Brazil
B. Li, M. Nami, and J. Han
Electrical Engineering, Yale University, New Haven CT
V. Meyers and S. Shahedipour-Sandvik
Nanoscale Science and Engineering, SUNY Polytechnic Institute, Albany NY

Although silicon-based electronics are used to power light-emitting diodes and electric vehicles, their utility in high power applications is limited by a low breakdown voltage. The most promising alternative power devices consist of vertical GaN devices, which require selected-area doping and/or regrowth. In this work, we use elastic-recoil detection analysis (ERDA) in conjunction with SIMNRA simulations to determine the depth-dependent [H] at p-GaN/i-GaN interfaces prepared without (“continuous”) and with ex-situ ambient exposure (“ex-situ”) and/or chemical etching (inductively-coupled plasma, “ICP etched”). For ERDA, 2.5 MeV He⁺ ions were delivered at an angle of 70° to the sample surface normal, and recoiled H was collected by a solid-state detector situated at 30° with respect to the incident ion direction. Simultaneously, backscattered He⁺ was collected with the RBS detector situated at 170° with respect to the incident ion direction. To validate the ERDA-SIMNRA data analysis approach, we quantify the depth-dependent [H] in deuterium-implanted GaN, taking into account surface water adsorption. For the p-GaN/i-GaN interfaces, ERDA data consisting of normalized H yield (right y-axis), and [H] (left y-axis) as a function of depth is shown in figure (a). On all surfaces, [H] > 1.0 × 10²¹/cm³, due to the presence of 3-10 nm of adsorbed water, is observed. In addition, [H] ~ 2.0 × 10²⁰/cm³ is observed at depths of 300 nm for all structures. Interestingly, for “ICP-etched”, [H] ~ 1.0 × 10²¹/cm³ is observed at a depth of 350 nm, presumably related to the ICP-etching process. It is interesting to note that commercially-performed Secondary Ion Mass Spectroscopy (SIMS) measurements/analysis, shown in figure (b), were unable to detect the significant interfacial [H].



For “Continuous”, “Ex-situ”, and “ICP etched” GaN, in comparison to a GaN substrate: (a) [H] vs. depth/energy, with Hydrogen yield (counts) on right axis (b) SIMNRA simulations and SIMS data.

IRRADIATION STABILITY OF PHOSPHATE AS A WASTE FORM HOST FOR ACTINIDES

K. Sun¹, G. S. Was²

¹Department of Materials Science and Engineering, University of Michigan

²Department of Nuclear Engineering and Radiological Sciences, University of Michigan

To establish the radiation tolerance of phosphate as a waste form host for actinide, a single crystal sample of $\text{Rb}_3\text{Nd}(\text{PO}_4)_2$ was irradiated at room temperature with a flux of $1.2 \times 10^{14} \text{ Xe}^{3+}/\text{m}^2\text{s}$ (damage rate of $3.7 \times 10^{-5} \text{ dpa/s}$) resulted in complete amorphization by 0.22 dpa, Figure 1. By quantitatively extracting the diffraction intensities from the series of SAED patterns taken at different damage levels, the volume fraction of amorphous phase at different damage levels was obtained. The dose to amorphization is similar to that for analcime zeolite.

The nano-crystal phosphate produced by heating the $\text{Rb}_3\text{Nd}(\text{PO}_4)_2$ to 1473 K was irradiated under the same conditions and required a higher dose to amorphization ($\sim 0.52 \text{ dpa}$) compared with the single crystalline $\text{Rb}_3\text{Nd}(\text{PO}_4)_2$. The amorphization dose is higher than those for analcime zeolite and similar to that for natural zircon. In both cases, amorphization is believed to be caused by disruption of the crystalline structure by displacement cascades. The higher amorphization dose for the nanocrystalline sample is likely due to the large grain boundary area that acts to absorb and annihilate mobile defects during irradiation.

Research was conducted by the Center for Hierarchical Waste Form Materials (CHWM), an Energy Frontier Research Center (EFRC). Research was supported by the U.S. Department of Energy, Office of Basic Energy Sciences, Division of Materials Sciences and Engineering under Award DE-SC0016574.

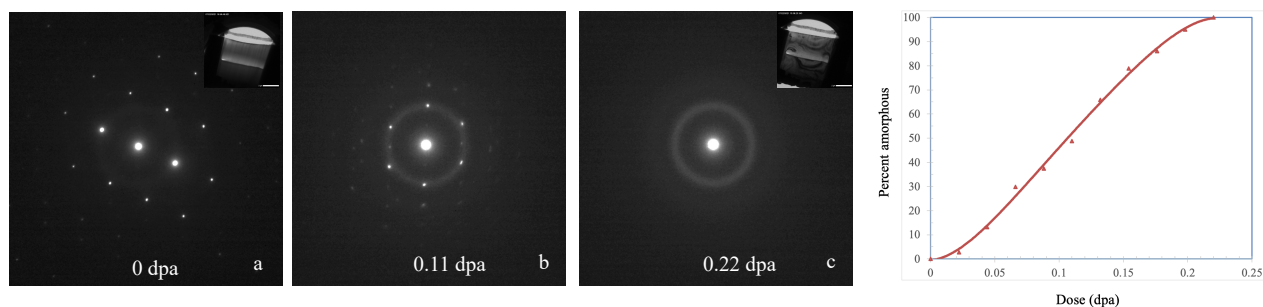


Figure 1. Series of SAED patterns showing the crystal to amorphous transition in $\text{Rb}_3\text{Nd}(\text{PO}_4)_2$ with increasing radiation damage and resulting amorphous percentage as a function of dose. The insets in (a) and (c) are BF images.

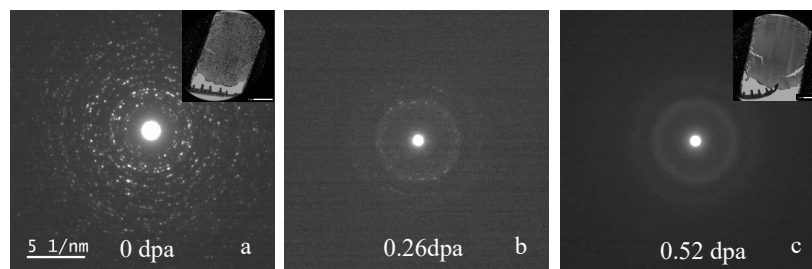


Figure 2. A series of SAED patterns showing the crystal to amorphous transition of the nanocrystalline Rb-phosphate at 0 dpa, 0.26 dpa and 0.52, dpa, respectively. The insets in (a) and (c) are BF images.

CALIBRATING SPUTTER TARGET DEPOSITION RATES

A. Ansari¹, B. Torralva², S. Yalisove^{1,3}

¹Department of Applied Physics, University of Michigan

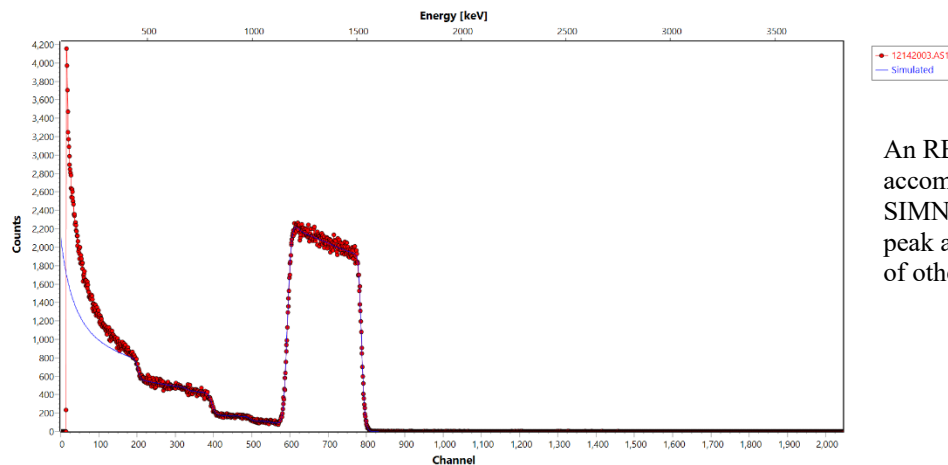
²Department of Climate and Space Sciences, University of Michigan

³Department of Materials Science and Engineering, University of Michigan

Finding the deposition rate of a sputtering system is valuable to precisely deposit films of a prescribed thickness. Calibration of a sputter target should also be performed when working conditions in the system have changed. This should also be done over the lifetime of the target, as the target has a different thickness on its active area as it is depleted by deposition. High sensitivity and low error techniques are preferred to perform calibration, and Rutherford Backscattering Spectrometry (RBS) affords these criteria.

2 MeV He⁺ ions were incident on nickel (Ni), copper (Cu), and molybdenum (Mo) films deposited using various sputter targets. A detector at 175° was used to collect backscattered ions. SIMNRA was used to model and fit the collected spectrum. A sputtering rate of 1.1 A/s was calculated for Ni, 3.09 A/s for Mo, and 5.37 A/s for Cu.

This work is sponsored by the Air Force Office of Scientific Research Contract Number FA9550-16-1-0312.



An RBS spectrum with an accompanying fit obtained from SIMNRA. The thickness of the peak as well as the concentrations of other elements were extracted.

THE DEVELOPMENT OF NEW CARBON AND HYDROGEN APATITE REFERENCE MATERIAL FOR STANDARDIZING MICRO-ANALYTICAL MEASUREMENTS

J. Hammerli^{1,2} and F. Naab³

¹Institute of Geological Sciences, University of Bern, Baltzerstrasse 1+3, CH-3012 Bern

²School of the Environment, Washington State University, Pullman, WA

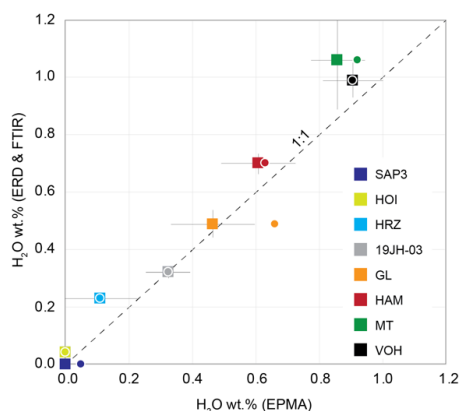
³Department of Nuclear Engineering and Radiological Sciences, University of Michigan

In this project we characterized the absolute carbon and hydrogen compositions of new natural apatite ($\text{Ca}_5(\text{PO}_4)_3(\text{F}, \text{Cl}, \text{OH})$) reference materials. Determining the absolute concentrations of hydrogen and carbon in a range of apatite minerals is key in order to use them as standards to normalize measurements carried out by micro-analytical instruments, such as Fourier-Transform Infrared Spectroscopy (FTIR), Electron Probe Micro-Analyzer (EPMA), or Secondary Ion Mass Spectrometry (SIMS). Absolute C and H concentrations in apatite were measured via ERD and NRA measurements, respectively.

ERD measurements were conducted via the 1.7 MV Tandetron accelerator. A 2.5 MeV He^{++} ion beam is used to impact the polished apatite surface from which H ions are released. Two detectors simultaneously collect the ERD and Rutherford back-scattering (RBS) spectra. The number of particle incidents on the sample during the acquisition of the ERD spectrum is measured via the RBS spectrum. A 12.5 μm Kapton ($\text{H}_{10}\text{C}_{22}\text{N}_2\text{O}_5$) film is used in front of the ERD detector to filter out ions heavier than H. Also, a Kapton polyimide foil is used as the H standard to determine the ERD detector solid angle ($\Delta\Omega$).

NRA via the 1.7 MV tandem accelerator was used to determine absolute carbon concentrations in apatite. A high-energy beam (1.4 MeV) of deuteron (^2H) particles is used to bombard the polished apatite surface to activate the ^{12}C (d,p) ^{13}C nuclear reaction ($^{12}\text{C} + ^2\text{H} \rightarrow ^{13}\text{C} + ^1\text{H}$). As the deuteron beam interacts with the sample, ^2H particles react with the target nucleus of carbon (^{12}C), converting the target nucleus to a new nucleus (^{13}C), while releasing ^1H as a reaction product with a specific amount of energy. The liberated ^1H ions are subsequently detected in the Si charged-particle detector, set at a scattering angle of 160° with a 15 keV energy resolution.

The quantification of absolute C and H in a range of apatite minerals and their use as standard reference material led to the development of a new analytical approach for in situ CO_2 and H_2O determination by ATR-FTIR in natural apatite in Earth materials (Hammerli et al., 2021). Besides the development of this new method, apatite grains measured for absolute C and H allowed for the first-time in-depth testing of the accuracy of current routine practices for the determination of H_2O in apatite. The vast majority of H_2O determinations in apatite are based on Electron Probe Micro-Analyser (EPMA) measurements, which do not record CO_2 concentrations. Our data show that the EPMA method and current stoichiometric approaches provide an accurate estimate of H_2O contents in apatite (figure).



H_2O determined by ERD and FTIR vs. H_2O constrained by the stoichiometry of apatite based on EPMA measurements. Square symbols represent stoichiometric H_2O calculation when CO_2 contents of apatite are considered and round symbols show H_2O determination when CO_2 contents are ignored. Uncertainties are 2SD of multiple ERD measurements or FTIR analyses perpendicular to the c-axis across a grain of the respective sample (2SD are the same for both symbol types) (modified from Hammerli et al., 2021).

MICROSTRUCTURAL EVOLUTIONS UNDER ION IRRADIATION LEADING TO THE SWELLING OF THE AIM1 ALLOY

A. Bermont¹, A. Deschamps², M. Jublot¹, A. Courcelle¹, D. Menut³

¹CEA Saclay- Semi- LM2E, F-91191, Gif sur Yvette, France

²Univ.Grenoble Alpes, CNRS, Grenoble INP2, SIMaP, F-38000, Grenoble, France

³Synchrotron SOLEIL, L'Orme des Merisiers, Saint Aubin BP48, Gif-sur-Yvette Cedex 91192, France

Ti-stabilized 15%Cr-15%Ni stainless steels such as the AIM1 steel developed by CEA in France are currently the reference material for fuel-pin cladding of GEN-IV sodium-cooled fast reactors. The main issue is to control their evolution during irradiation in terms of swelling and more generally the distribution of chemical species. The microstructural and chemical properties at high dose (>100 dpa) that lead to swelling, are strongly dependent on the irradiation temperature, the initial microstructure and the first steps of the microstructural evolution under irradiation, which have been studied in this PhD work.

Neutron irradiation can be simulated by ion and proton irradiation, which are more practical and enable analytical study of irradiation parameters. This work presents a multi-scale microstructure analysis of the effect of ion and proton irradiation on AIM1, with two initial microstructures having different densities of crystalline defects: solution annealed (low defect density) and 20% cold-worked (high density of dislocations and mechanical twins). In order to simulate irradiation effect on AIM1 microstructure, several experiments were carried out. First, Ni²⁺ ion irradiations were performed at 450°C and 550°C at two fluences to get several doses ranging from 3 dpa to 10 dpa at a depth of 1 µm. A second irradiation campaign was performed at MIBL laboratory with protons at 450°C to obtain a damage of 2 dpa and achieve a greater depth of damage (~10 µm) suitable for synchrotron analysis (diffraction analysis and SAXS technique). TEM and APT studies are in progress to compare ion and proton irradiations and to get relevant information on microstructure evolution at nanometric and atomic scale.

IN-SITU PROTON IRRADIATION-CORROSION EXPERIMENT OF BETA-SILICON CARBIDE AT 300°C IN PURE WATER

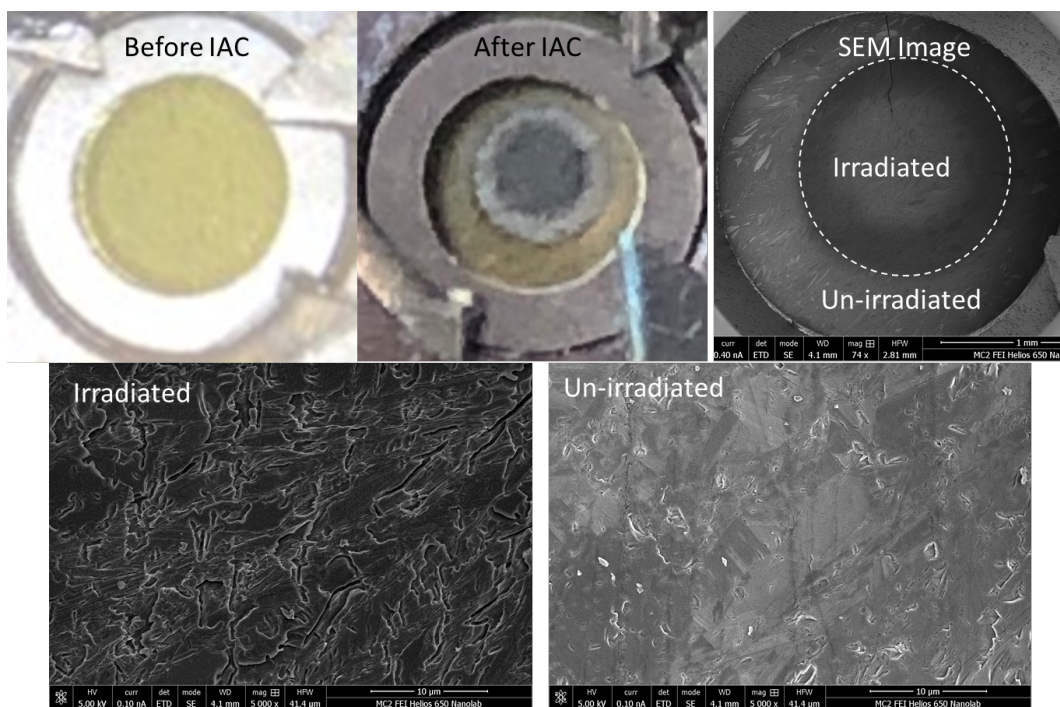
P. Wang¹, G. S. Was¹

¹Department of Nuclear Engineering and Radiological Sciences, University of Michigan

The objective of this project is to develop a mechanistic understanding of the hydrothermal corrosion behavior of monolithic SiC and SiC/SiC composites in the LWR environment under the influence of water radiolysis products and radiation damage. The project focus on the radiation and radiolysis effects of SiC hydrothermal corrosion on chemical vapor deposited (CVD) β -SiC variants (3C-SiC). The effects of water chemistry and radiolysis products on hydrothermal corrosion will be evaluated via in-situ irradiation-corrosion experiments. The extensive post-test characterization will be performed to determine the dissolution rate of the samples, surface morphology, surface chemical composition, and depth profile of SiC from the surface, etc.

In the figure, an arial shot of the SiC disc before and after in-situ irradiation-corrosion (IAC) exposure shows the difference between the irradiated and un-irradiated region of the SiC disc.

This research was supported by the Department of Energy, Federal Grant #: DE-NE0008781.



3C-SiC disc sample before and after IAC exposure, SEM image of sample surface (top right) shows the irradiated region (lower left) with more GB attacks and un-irradiated region (lower right) was virtually free of corrosion.

SILICON ION IRRADIATION OF BETA-SILICON CARBIDE AT 300°C

P. Wang¹, G. S. Was¹,

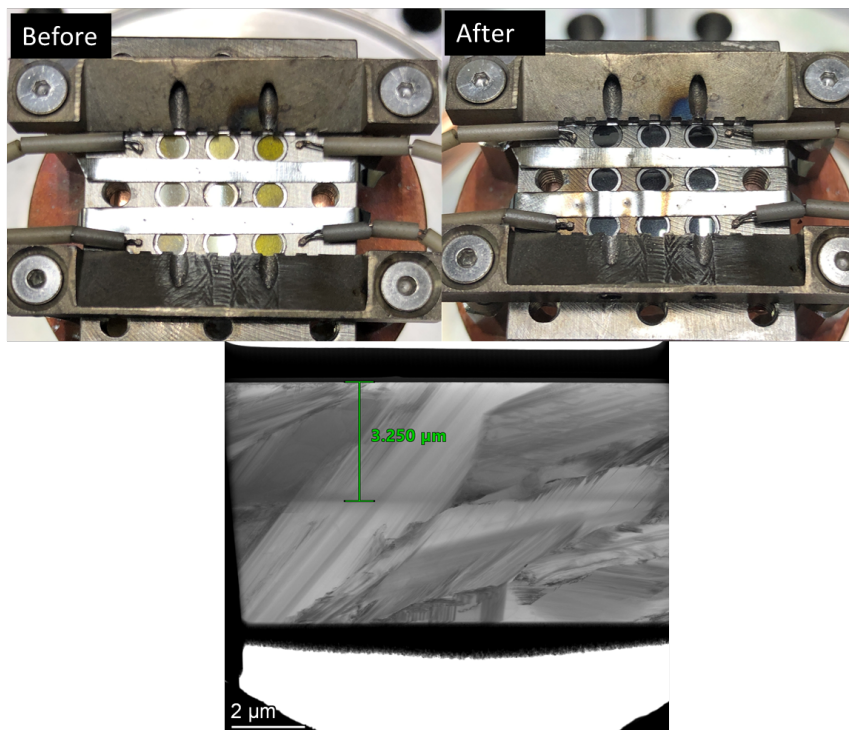
¹ Department of Nuclear Engineering and Radiological Sciences, University of Michigan

The objective of this project is to develop a mechanistic understanding of the hydrothermal corrosion behavior of monolithic SiC and SiC/SiC composites in the LWR environment under the influence of water radiolysis products and radiation damage. The project focus on the irradiation damage on the microstructure and microchemistry evolution of SiC under self-ion irradiation. The irradiated microstructure will be compared to in-reactor irradiated samples to validate if self-ion can produce the correct microstructure observed on neutron irradiated SiC. SiC discs of 3mm diameter and thickness of 50 μ m were loaded in a sample holder and irradiated with 7.5MeV Si²⁺ ions at 300°C to a damage level of 2 and 12 dpa to match neutron irradiated SiC samples.

After microstructure characterization and analysis, these re-irradiated samples will be used in studies regarding the radiolysis effects of SiC hydrothermal corrosion on chemical vapor deposited (CVD) β -SiC variants (3C-SiC). The effects of water chemistry and radiolysis products on hydrothermal corrosion will be evaluated via in-situ irradiation-corrosion experiments on these pre-irradiated samples. Due to the unique microstructure feature of the Si³⁺ irradiation, the implantation of the silicon ion would induce a damage peak at $\sim 3.25 \mu\text{m}$, which can be used as a marker layer to track the SiC dissolution during corrosion test.

In the figure, SiC discs are loaded into a 3x3 array sample holder, before irradiation the samples are transparent yellow color, after irradiation the samples loss transparency and turned black. The damage peak can be clearly observed in the TEM image at 3.25 μm below the surface.

This research was supported by the Department of Energy, Federal Grant #: DE-NE0008781.



3C-SiC disc samples before and after self-ion irradiation, lower TEM image shows the FIB lift-out taken from the as-irradiated SiC disc, with a damage peak close to 3.25 μm below the irradiated surface.

ASSESSMENT OF SHADOW CORROSION MITIGATION COATINGS USING IN-SITU PROTON IRRADIATION-CORROSION TESTS (2020-I)

P. Wang¹, G. S. Was¹, K. Nowotka²

¹Department of Nuclear Engineering and Radiological Sciences, University of Michigan

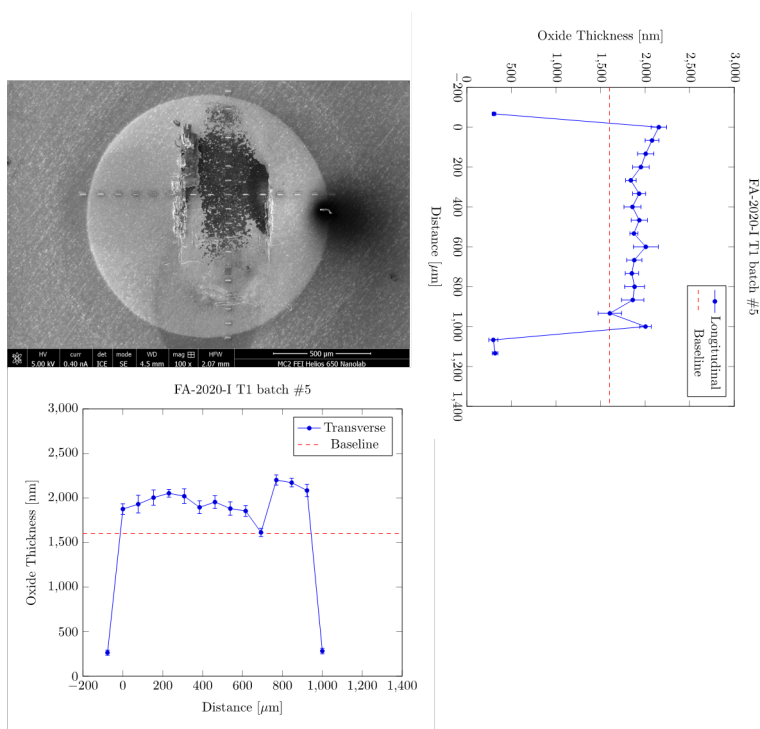
²Framatome GmbH

Shadow corrosion, as a type of irradiation-assisted galvanic corrosion between dissimilar metals, the shape of the component is often reproduced in the shape of an area of enhanced corrosion, suggestive of shadow casted by the component on the zirconium alloy surface. Shadow corrosion is also closely related to the channel bowing phenomena, which resulted in control blade interference due to channel distortion.

Several mechanisms have been proposed to explain the appearance of shadow corrosion, and the majority are related to the electrochemical nature of the Zircalloys. However, to date, shadow corrosion has only been observed on samples exposed in reactor. This implies the possible mechanisms by which radiation assists the shadow corrosion process; (1) by increasing the electrical and ionic conductivity of the oxide on Zr alloy, (2) by increasing the oxidizing species at the metal/oxide interface through creating radiolysis products. This project was aimed to use the existing spring-loaded wire design, to assess the durability and effectiveness of the newly developed shadow corrosion mitigation coatings on Inconel 718.

In the figure, where shadow corrosion mitigation coating has been applied to the Inconel 718 wire were tested, and the results shown no acceleration of oxide growth underneath the Inconel wire in both directions. The baseline case represents the oxide thickness resulted from a proton irradiation without the Inconel 718 counter-electrode attached.

This research was supported by the Framatome GmbH, Contract No.GF01/1020039285.



Oxide thickness profile across the in-situ irradiated-corrosion region, the resulting oxide thickness was compared between a coated (data points in blue) and baseline result (dash line in red).

IN-SITU PROTON IRRADIATION-CORROSION EXPERIMENT OF PRE-IRRADIATED ZIRCALOY-4

P. Wang¹, G.S. Was¹, B. Kammenzind², E. Lacroix³

¹Department of Nuclear Engineering & Radiological Sciences, University of Michigan

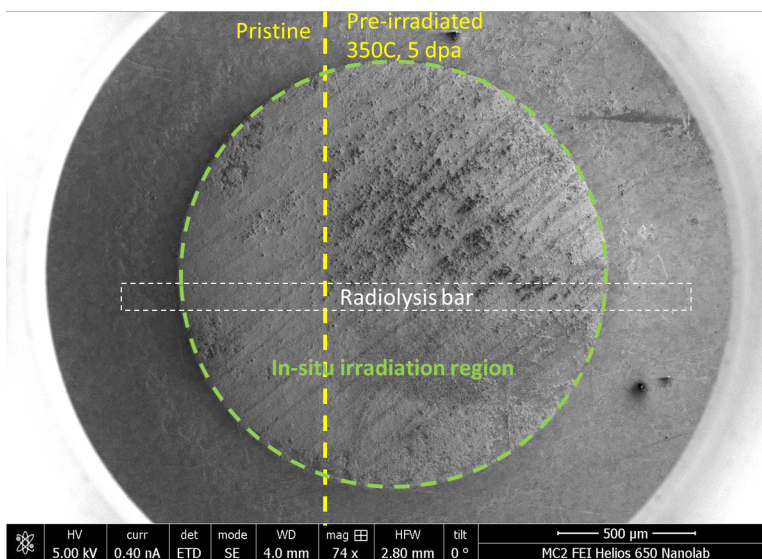
²Navel Nuclear Laboratory

³Framatome Inc

The mechanistic understanding of zirconium alloy corrosion in out of reactor testing has advanced the state-of-the-art of the field and provided insights in identifying promising alloys for use in reactors under extreme service duty conditions. However, despite similarities between autoclave and in-reactor corrosion that allow the use of unirradiated material information and testing to identify potential alloys for service, processes that occur in the reactor are quantitatively and qualitatively different than those in an autoclave environment.

This work assesses the corrosion behavior of proton pre-irradiated Zircaloy-4 sample in simulated LWR reactor environments. Proton pre-irradiations have been performed on Zircaloy-4 samples via isothermal temperature irradiation at 350 °C or two-step proton irradiation to enhance the amorphization of and Fe loss from the laves phase $Zr(Fe,Cr)_2$ precipitates. The as-irradiated microstructures were characterized in an earlier publication. In-situ irradiation-corrosion experiments were then performed on the pre-irradiated samples at 320°C in pure water with various dissolved gases, including hydrogen, nitrogen and argon, etc. The aim of this systematic investigation of corrosion under influence of active irradiation, existing defect damage, and radiolysis products would offer better understand of separate and combined effects on corrosion.

This work was supported by the Navel Nuclear Laboratory and Framatome Inc.



SEM images of Zry-4 sample surface after in-situ proton irradiation-corrosion experiment, the in-situ irradiation area (green circle) covers both the pristine and pre-irradiated region of the Zry-4 sample.

Cr PATTERNED In625 FOR IN-SITU TEM MOLTEN SALT CORROSION STUDIES

J. Bankson¹, Dr. P. Pragnya¹, Prof. D. Gall¹, Prof. R. Hull¹

Collaborators: Dr. Emily Liu & group² and Dr. Jinsuo Zhang & group³

¹Department of Material Science and Engineering, Rensselaer Polytechnic Institute

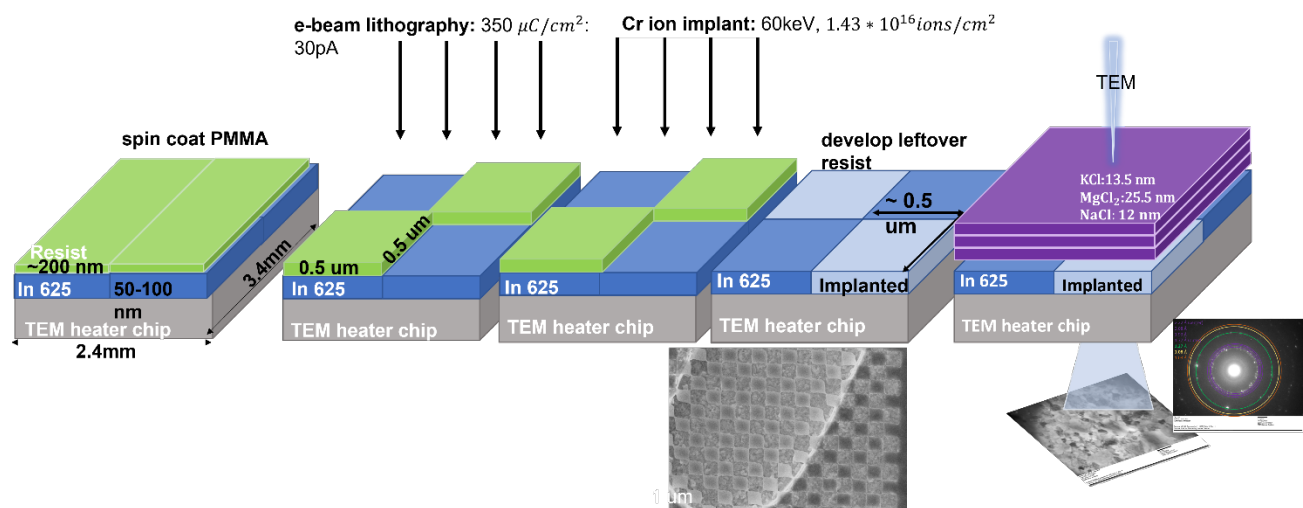
²Department of Mechanical Engineering, Rensselaer Polytechnic Institute

³Department of Nuclear Engineering, Virginia Technical Institute

The next generation of Concentrated Solar Power plants (CSP) will have increased capacities because of molten chloride salts which are cheaper, have lower eutectic melting points, and higher thermal stability range. This project funded by the U.S Department of Energy is to improve the current understanding of corrosion between molten chloride salts (NaCl – MgCl₂ – KCl) and the alloy, Inconel 625 (In625). There has been evidence in literature of Cr leading to more severe corrosion of the alloy because of its preferential depletion to form voids, as well as a surface oxide which is broken apart due to the formation of volatile Cr chlorides.

Our objective was to increase local area concentrations of Cr in the In625 through ion implantation so that we can compare corrosion response of standard vs Cr-enriched regions in our in-situ transmission electron microscopy (TEM) experiments. To create patterns of implanted versus non-implanted regions, electron beam lithography was used to create a polymer resist mask above a 75nm film of In625. Figure 1 shows the 0.5 x 0.5um grid pattern. The exposed regions were ion implanted with Cr. SRIM calculations were performed to inform the choice of energy and dose (60vkeV, 1.43 x 10¹⁶ ions/cm²) so that the max concentration occurs within the In625 film. After the patterned implantation, the TEM sample undergoes a removal process of the polymer mask, electron beam deposition of 3 layers of chloride salts (NaCl, 12 nm – MgCl₂, 25.5 nm – KCl, 13.5 nm), and high-temperature molten salt corrosion with a microenvironmental cell TEM holder.

Funding: Department of Energy (DOE) (Grant Number- DoE EERE De-EE0008380)



Schematic for the process of electron beam patterning of alloy In625 (SEM micrograph), ion implantation, and the in-situ TEM corrosion experiment where 3 salts are melted to form a ternary eutectic composition.

THE ORIGIN OF EXCEPTIONAL IASCC RESISTANCE OF THE ADDITIVELY-MANUFACTURED STAINLESS STEEL AFTER HOT ISOSTATIC PRESSING

X. Lou¹, J. Yang¹, M. Song²

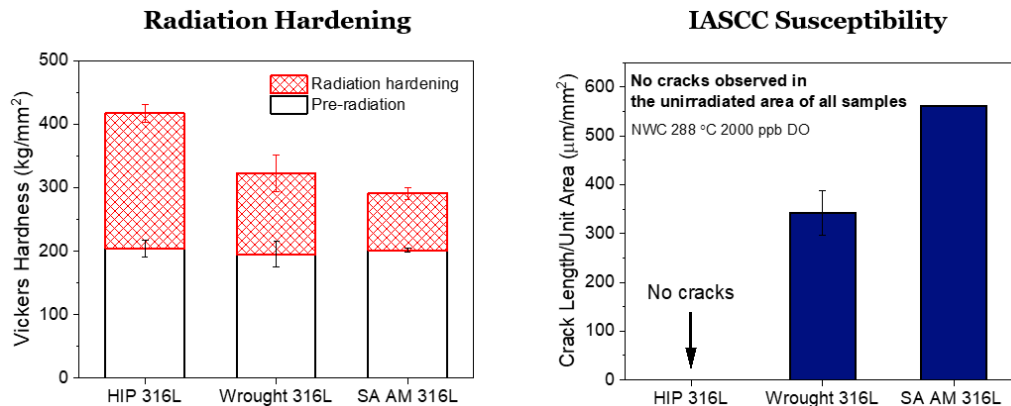
¹Department of Mechanical Engineering, Auburn University

²Department of Nuclear Engineering and Radiological Sciences, University of Michigan

This NSUF RTE project seeks to conduct proton irradiation at the Michigan Ion Beam Laboratory to confirm and understand the exceptional irradiation-assisted stress corrosion cracking (IASCC) resistance of the additively-manufactured (AM) 316L stainless steel after hot isostatic pressing (HIP) process. This phenomenon was reported through the completed DOE NEET project (DE-NE0008428) (M. Song, et al., JNM, 513, pp 33-44 (2019)). The HIPed AM 316L stainless steel exhibited surprisingly high resistance to IASCC initiation than its wrought counterpart. Material characterization showed both materials shared very similar alloy chemistry and grain structure, as well as a similar amount of slip channels along the grain boundaries after the slow strain rate test (SSRT).

A different heat of AM 316L SS was fabricated by Concept Laser M-lab laser powder bed fusion (LPBF) system, and later heat-treated at 1100 °C for 2 hours to obtain fully recrystallized grain structure. Both mini tensile specimens and TEM specimens were machined for radiation study and testing. The proton irradiation with 2 MeV protons was conducted in the Michigan Ion Beam Laboratory. Irradiations were performed at a temperature of 360 °C with a damage level of 2.5 dpa (Kinchin-Pease calculation) at ~10 µm below the surface. A total proton range of ~20 µm was achieved. Experiments lasted ~90 h, resulting in the calculated damage rate of 6.9×10^{-6} – 8.7×10^{-6} dpa/s. After radiation, the tensile bars were tested at Auburn University for IASCC initiation by constant extension rate test (CERT). The CERT test was performed in Boiling Water Reactor (BWR) environment at 288 °C and 2 ppm dissolved oxygen. A strain rate of 1×10^{-7} s⁻¹ was applied until a plastic strain of 4% was reached.

This research was supported by the U.S. Department of Energy (DOE) Nuclear Science User Facilities (NSUF) experiment under DOE Idaho Operations Office Contract DE-AC07-05ID14517.



Radiation hardening and IASCC susceptibility of the materials evaluated in this project.

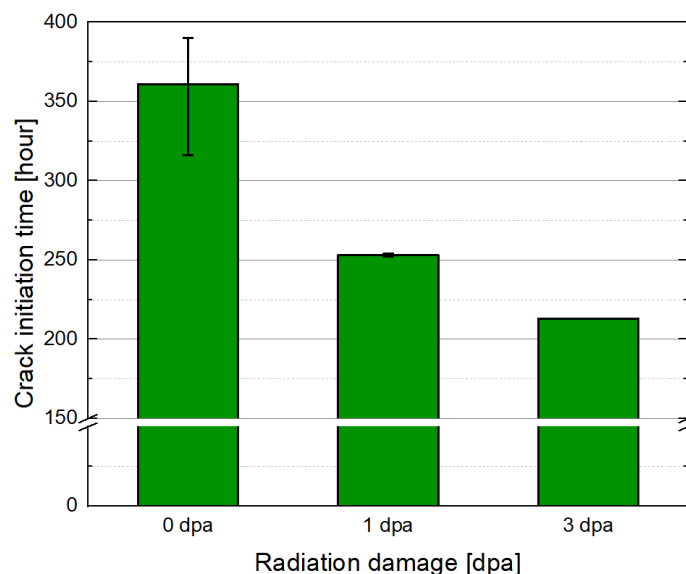
PROTON IRRADIATION EFFECT ON CRACK INITIATION BEHAVIOR OF 304L STAINLESS STEEL

J. Ham, S.C. Yoo, and J.H. Kim

Department of Nuclear Engineering, Ulsan National Institute of Science and Technology

Austenitic stainless steel has been widely used in primary circuits of pressurized water reactor. Especially type 304 and 316 stainless steels are the main materials of the reactor internal structures supporting the reactor core. These kinds of structural components are located close to the nuclear fuel of reactor and are irradiated by neutron which causes severe problem irradiation assisted stress corrosion cracking (IASCC). Most of SCC studies have used U-bend specimen in various environment. But U-bend test has a limitation related to its long experimental period. To overcome this weakness, slow strain rate test (SSRT) or constant elongation rate test (CERT) are used which are a kind of acceleration test observing fracture surface. However, in point of view of IASCC, the effect of irradiation is concentrated in the shallow irradiated surface. Thus, it is hard to investigate the effect of irradiation using fracture surface observation method when it comes to deal with crack initiation. In this study, IASCC susceptibility of 304L stainless steel was investigated by conducting SSRT experiments combining with direct current potential drop (DCPD) methodology to detect the exact moment of crack initiation using unirradiated, 1 dpa, and 3 dpa proton irradiated samples respectively.

Proton irradiation had been done from Michigan Ion Beam Laboratory (MIBL) using proton whose beam energy was 2 MeV to a damage level of 1 and 3 dpa at 360 °C. Each SSRT experiment was conducted until the moment when some remarkable electrical signal was detected from DCPD system. According to the result of experiments whose test environment had been controlled as similar as pressurized water reactor primary circuit, the average crack initiation time of unirradiated samples was about 361 hours, and that of 1 dpa and 3 dpa samples were 253 hours and 213 hours respectively. Proton irradiation did not change the bulk sample's mechanical properties since it affected just shallow depth from the surface, about 20 μm , but the micro-crack initiated on the surface could be detected precisely by DCPD methodology. The additional experiments with 7 dpa sample are now in progress. The detail results will be dealt from journal paper.



Comparison of crack initiation time measurement depending on the level of radiation damage. The crack initiation happened earlier with unirradiated sample, and the crack initiation time became shorter when the damage level increased from 0 to 3 dpa.

IN-SITU MICROSTRUCTURE OBSERVATION OF OXIDIZED SiC LAYER IN SURROGATE TRISO FUEL PARTICLES UNDER KRYPTON ION IRRADIATION

Y. J. Cho¹, K. Sun², G. S. Was^{2,3}, Kathy Lu¹

¹Materials Science and Engineering, Virginia Tech, Blacksburg, Virginia

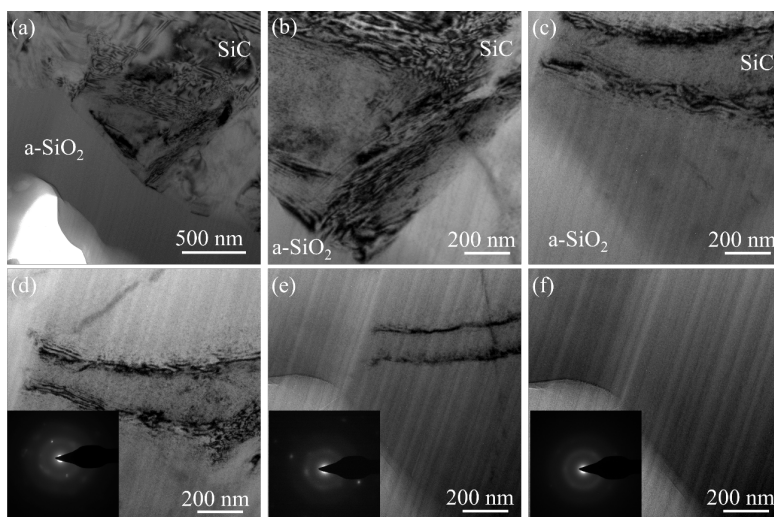
²Materials Science and Engineering, University of Michigan

³Nuclear Engineering and Radiological Sciences, University of Michigan

Silicon carbide (SiC) is a promising fission barrier material in tri-structural-isotropic (TRISO) particles owing to its high thermal conductivity, mechanical properties, and environmental stabilities. The dense SiC layer in the TRISO fuel particles acts as a main structural component to retain migration of gaseous and metallic fission products insufficiently blocked by other inner layers. In accidental scenarios of high temperature gas-cooled reactors, both oxidation of and irradiation to the SiC layer in TRISO fuel particles can change the microstructure and integrity of the fuel elements. The SiO₂ layer formed on the SiC surface is initially amorphous and can transform into crystalline depending on temperature and time.

In the present study, microstructure and defect evolution in the oxidized SiC layer of surrogate TRISO fuel particles under 1.2 MeV krypton ion irradiation was observed by in-situ transmission electron microscopy. The SiC layers oxidized in water vapor at 1200 °C were irradiated at room temperature and 800 °C and at damage levels of 0.28–11.2 dpa, respectively. SiC and SiO₂ were found to still be in their crystal structures at the damage level of 11.2 dpa at 800 °C, while SiC was observed to have been amorphized at only 0.56 dpa irradiation at room temperature. The defect number density at 800 °C was an order of magnitude lower than that in the sample irradiated at room temperature. Also, crystalline SiO₂ had higher radiation resistance compared to SiC. A defect reaction rate theory was utilized to understand the fundamental defect evolution process and irradiation resistance difference.

This work was supported by the Office of Nuclear Energy of Department of Energy (grant no. DE-NE0008808). We thank Oak Ridge National Laboratory for sharing the surrogate TRISO fuel particles (AGRBW-4A2).



Bright-field TEM images and SAED patterns of the SiC and oxide layers irradiated by 1.2 MeV Kr ions at RT with a damage level of (a) 0, (b) 0.28, (c) 0.56, (d) 1.12, (e) 1.68, and (f) 2.8 dpa, respectively.

RADIATION TOLERANCE OF ADDITIVELY NANOSTRUCTURED ALLOY-2 (ANA2) FOR ADVANCED REACTORS

T.M.K. Green¹, K. G. Field¹, W. Zhong², L. Tan²

¹Department of Nuclear Engineering and Radiological Sciences, University of Michigan

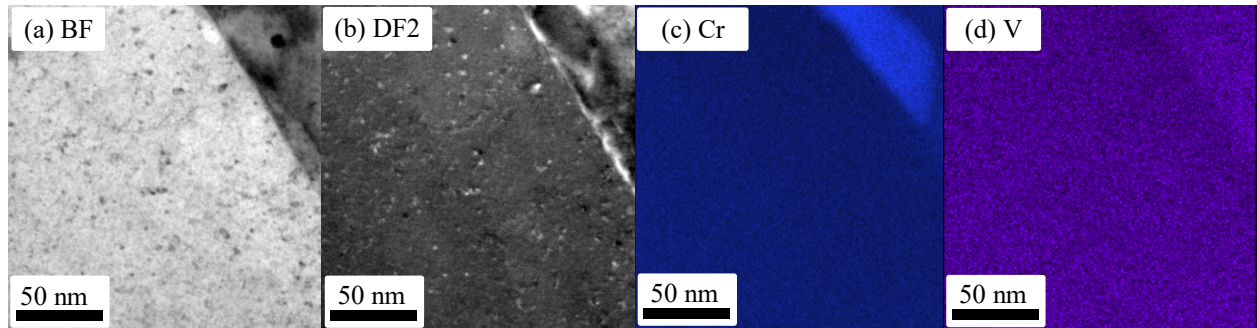
²Oak Ridge National Laboratory

The objective of this project is to observe the dynamic behavior of MX (M=V/Cr, X=N) nanoprecipitates and helium in a novel ferritic/martensitic (F/M) alloy, designated as Additively Nanostructured Alloy-2 (ANA2a), through high fidelity ion irradiation experiments (Zhong et al. 2021). To date, separate effects testing of the variables of temperature and dose rate have been studied with irradiation experiments (Table). Temperature effects on nanoprecipitates is being investigated via electron microscopy after completion of a single ion beam irradiation series started in 2020 and finished in 2021 (irradiations 1.1B and 1.1C). Another series of experiments is underway isolating effects of dose rate (irradiations 1.2A and 1.2B). All irradiations achieved a nominal damage of 50 dpa, with varying dose rate values. Temperatures ranged from 300-500°C.

Parameters	Temperature Series		Dose Rate Series	
	Irradiation 1.1B	Irradiation 1.1C	Irradiation 1.2A	Irradiation 1.2B
Ions	9 MeV Fe ³⁺	9 MeV Fe ³⁺	9 MeV Fe ³⁺	9 MeV Fe ³⁺
Displacements per atom (dpa)	50	50	50	50
Dose rate (dpa/s)	10 ⁻⁴	10 ⁻⁴	10 ⁻³	5×10 ⁻⁴
Temperature (°C)	500	300	400	400
Samples irradiated	ANA2a, F82H, AM-HT9	ANA2a, C81, C91, F82H	ANA2a, ANA2b, C81, C91	ANA2a, ANA2b, C81, C91
Beamline/accelerator	BL2 Wolverine, Peabody source			

For each irradiation, four samples of F/M steel bars each 10^L × 1.5^H × 1.5^W mm³ were machined from bulk specimens. Pressure, temperature, and beam currents were recorded during the irradiation experiments. A defocused beam 24mm² in area was used. The figure shows scanning transmission electron microscopy (STEM) micrographs and STEM-EDS elemental maps of V and Cr for irradiation 1.1C. The initial high density of (V,Cr)N nanoprecipitates present in unirradiated ANA2a dissolved during irradiation.

Research and development efforts associated with the DED technology was supported by the Laboratory Directed Research and Development Program of Oak Ridge National Laboratory (ORNL) and the U.S. Department of Energy (DOE), Office of Nuclear Energy (NE), Advanced Fuels Campaign, under Contract no. [DE-AC05-00OR22725](#) with UT-Battelle, LLC. Samples from these efforts were procured, irradiated, and characterized as part of an FES sponsored Early Career Award (DE-SC0021138).



(a) STEM BF, (b) STEM dark field (DF2), (c) elemental map of Cr, and an (d) elemental map of V taken at a depth of 1,100-1,300 nm after irradiation at 500°C (Irradiation 1.1C).

TEACHING

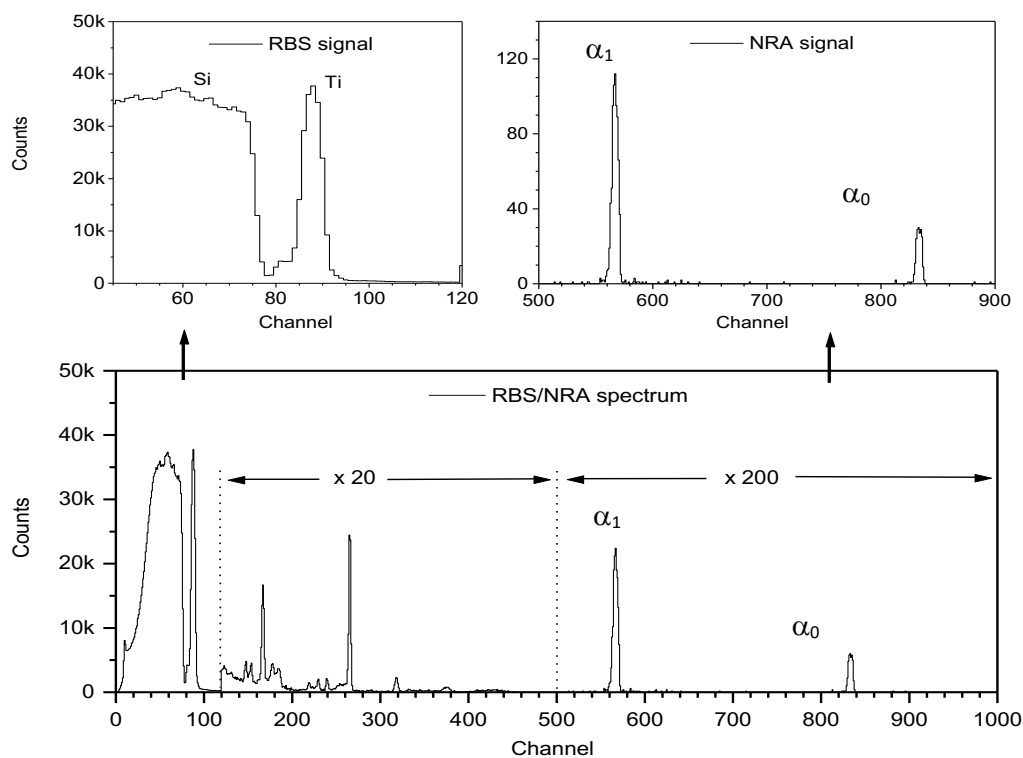
NERS 425 LABORTORY ON NUCLEAR REACTION ANALYSIS

M. Atzmon, F. Naab and O. Toader

Department of Nuclear Engineering and Radiological Sciences, University of Michigan

For one of the modules in the NERS 425 course, students conducted an experiment to determine the stoichiometry of a Ti_xN_y sample using the reaction between a deuterium particle and a nitrogen nucleus: $\text{N}^{14}(\text{d},\alpha)\text{C}^{12}$. Nuclear reaction analysis (NRA) is a well-established surface analysis technique. In this method, an energetic particle (deuterium – produced by the Tandem accelerator at MIBL) interacts with the nucleus of an N atom in the target to give a reaction product (α particle) that can be measured. The students also use the backscattered yield from an RBS experiment to determine the amount of Ti in the sample by implementing simulation codes like RUMP or SIMNRA with the given experimental spectrum.

In the first meeting, prior to the experiment, a short tutorial was given to the students on the accelerator, electronics, detectors, software, and vacuum components. After that, they worked independently with just the basic support from the MIBL staff (required in the setup of the ion beam and the collection of the spectra). The students decided on a few parameters of the experiment (beam energy, time for spectrum acquisition, etc.), and obtained spectra similar to the ones in the figure.



Typical RBS/NRA spectrum for the TiN film obtained during class. Conditions: beam energy: 1.4 MeV D^+ , solid angle 5 msr., detector angle 150° .

PUBLICATIONS AND PRESENTATIONS

Publications

1. E. Jossou, A. Schneider, C. Sun, Y. Zhang, S. Chodankar, D. Nykypanchuk, J. Gan, L. Ecker, S. Gill, “Unraveling the early-stage ordering of krypton solid bubbles in molybdenum: A multi-model study”, Journal of Physical Chemistry, 125 (2021): 23338.
2. C. Sun, C. Jiang, E. Jossou, M. Topsakal, S. K. Gill, D. J. Sprouster, L. E. Ecker, J. Gan, “Self-assembly of solid nanoclusters in molybdenum under gas ion implantation”, Scripta Materialia, 194 (2021): 113651.
3. C. Sun, “A short review of defect superlattice formation in metals and alloys under irradiation”, Journal of Nuclear Materials, 559 (2022): 153479.
4. Y.-J. Cho, K. Sun, G. Was, K. Lu, “In-situ microstructure observation of oxidized SiC layer in surrogate TRISO fuel particles under krypton ion irradiation”, Materials Today Physics, submitted.
5. K. Lu, S. Singh, “In-situ TEM study of Kr ion irradiation tolerance of SiFeOC nanocomposite,” Materials Physics and Chemistry, submitted.
6. S. Taller, G. VanCoevering, B. D. Wirth, G. S. Was, “Predicting structural material degradation in advanced nuclear reactors with ion irradiation,” Scientific Reports 11 (2021) 1-14.
7. D. Woodley, S. Taller, Z. Jiao, K. Sun, G. S. Was, “The Role of Helium Co-Injected Helium on Swelling and Cavity Evolution at High Damage Levels in Ferritic-Martensitic Steels”, Journal of Nuclear Materials 550 (2021) 152912.
8. P. Wang, J. Bowman, M. Bachhav, B. Kammenzind, R. Smith, J. Carter, A. Motta, E. Lacroix, G. Was, “Emulation of neutron damage with proton irradiation and its effects on Microstructure and Microchemistry of Zircaloy-4,” J. Nucl. Mater. 557 (2021) 153281.
9. C. Silva, M. Song, M. Wang, K. Holliday, K. Leonard, G. Was, J. Busby, “A Microscopic and Crystallographic Study of Proton Irradiated Alloy 718,” J. Nucl. Mater. 551 (2021) 15295.
10. P. Wang, S. Grdanovska, D. M. Bartels, G. S. Was, “Corrosion behavior of Ferritic FeCrAl Alloys in Simulated BWR Normal Water Chemistry,” J. Nucl. Mater. 545 (2021) 152744.

Presentations

1. C. Sun, “Defect superlattice in metals under irradiation” Annual User Meeting, Center of Integrated Nanotechnologies (CINT), Santa Fe, NM, September 2021.
2. C. Sun, “The role of anisotropy on the defect self-organization in metals under irradiation”, MS&T2021, Columbus, OH, October 2021.
3. K. Lu, S. Singh, “In-situ Temperature Dependent Ion Irradiation Tolerance of SiFeOC Nanocomposite,” 46th International Conference and Exposition on Advanced Ceramics and Composites (ICACC 2022), Daytona Beach, FL, virtual, January 23 - 28, 2022.
4. K. Lu, Y. J. Cho, “In-situ Microstructure Observation of Oxidized SiC Layer in Surrogate TRISO Fuel Particles,” 46th International Conference and Exposition on Advanced Ceramics and Composites (ICACC 2022), Daytona Beach, FL, virtual, January 23 - 28, 2022.\

5. S. Taller, "Solute Segregation and Precipitation Across Damage Rates in Dual Ion Irradiated T91 Steel," Materials in Nuclear Energy Systems 2021, Pittsburgh, PA, November 2021.
6. V. Pauly, "Effect of Helium Injection Rate on Cavity Microstructure in Dual Ion Irradiated T91 Steel," Materials in Nuclear Energy Systems 2021, Pittsburgh, PA, November 2021.
7. G. S. Was, "Application of Particle Accelerators to the Degradation of Materials in the Nuclear Reactor Core Environment," AccApp21, Washington DC, December 2021.
8. G. S. Was, "Ion Irradiation Capabilities of the Michigan Ion Beam Laboratory," Snowmass'21 - Irradiation Stations and Alternatives Workshop – June 2021
9. G. S. Was, "Impact of Radiation on Corrosion and SCC of Austenitic Stainless Steels," 1st Corrosion and Materials Degradation Web Conference, May 2021.
10. D. Farkas, G. S. Was, I. M. Robertson, "Grain Boundary Diffusion in Stainless Steel from Atomistic Simulations," TMS Annual Meeting, March 2021.
11. G. S. Was, M. Song, "Additively Manufactured 316L Stainless Steel for Nuclear Applications," TMS Annual Meeting, March 2021.
12. M. E. Parry, C. D. Judge, C. Sun, W. Jiang, B. Kombariah, G. S. Was, M. Daymond, J. A. Aguiar, T. D. Sparks, "Accelerated Study of Thermal and Irradiation Creep in Fe-based Multi-Principal Element Alloys," TMS Annual Meeting, March 2021.
13. G. Was, "Reactor Structural Materials: Matching Demanding Environments with Advances in Characterization," Workshop on Advanced Microscopy for Nuclear Fuels and Materials, Idaho National Laboratory, January 2021.